

THE PROPERTIES OF BUOYANT TURBULENT THERMALS AND PLUMES IN STILL AND CROSSFLOWING ENVIRONMENTS

by

G. M. Faeth^{*}, Z. Dai⁺, F. J. Diez[†], O. C. Kwon[‡] and R. Sangras^{**}
Department of Aerospace Engineering
The University of Michigan
Ann Arbor, Michigan 48109-2140

ABSTRACT

Recent studies of the structure and penetration properties of round buoyant turbulent thermals, starting plumes and steady plumes (denoted thermals, starting plumes and steady plumes in the following) in still and crossflowing unstratified uniform environments are reviewed, emphasizing conditions far from the source where the self-preserving flow approximation of turbulence can be applied to simplify correlation of flow properties. Studies of the structure of these flows are mainly limited to steady plumes in still environments finding that complete self-preserving behavior is dominated by flow radius properties and only is observed at distances greater than roughly 100 source diameters from the source, which is farther

from the source and yields narrower flows than previously thought.

Studies of flow penetration properties have considered thermals and starting plumes in both still and crossflowing environments. Measurements of these flows have involved salt water sources in fresh water environments which allows self-preserving conditions to be reached using compact experiments while still achieving large Reynolds numbers having practical interest. Experiments in still environments show that penetration properties approximate self-preserving behavior rather quickly, at 40 source diameters from the source, compared to the structure properties of steady plumes that only achieve self-preserving behavior at distances greater than 100 source diameters from the source. Observations of thermals and starting plumes in crossflow show that penetration in the crossflow direction satisfies the no-slip convection approximation whereas maximum penetration distances in the vertical and radial directions correlate in the same manner as the corresponding flows in still fluids, and achieve self-preserving behavior at similar conditions, which provides simple ways to estimate flow properties.

^{*}A.B. Modine Professor, Fellow AIAA, corresponding author; Tel:+1-734-764-7202; Fax: +1-734-936-0106;

E-mail: gmaeth@umich.edu (G.M. Faeth).

⁺Currently Lead Engineer, G.E. Aircraft Engines, Cincinnati, Ohio.

[†]Post-Doctoral Research Fellow, AIAA member.

[‡]Post-Doctoral Research Fellow. Currently Research Associate, University of Southern California, Los Angeles, California.

^{**}Post-Doctoral Research Fellow.

Copyright © 2002 by G.M. Faeth. Published by the American Institute of Aeronautics and Astronautics, Inc., with permission.

NOMENCLATURE

| | | |
|----------------|---|---|
| A_0 | = | source cross-sectional area |
| B_0 | = | source specific buoyancy force for round sources |
| \dot{B}_0 | = | source specific buoyancy flux for round sources |
| C_r | = | radial penetration coefficient |
| C_x | = | streamwise (vertical) penetration coefficient |
| C_y | = | crosstream (horizontal) penetration coefficient |
| d | = | diameter of the source |
| E_0 | = | entrainment constant, Eq. (17) |
| f | = | mixture fraction |
| $F(r/(x-x_0))$ | = | scaled variation of \bar{f} in the radial direction |
| Fr_0 | = | source Froude number |
| g | = | acceleration of gravity |
| k_f, k_u | = | plume width coefficients based on \bar{f} and \bar{u} |
| L | = | source passage length |
| l_f, l_u | = | characteristic plume radii based on \bar{f} and \bar{u} |
| l_M | = | Morton length scale for round sources |
| \dot{M}_0 | = | source specific momentum flux |
| n | = | time exponent |
| Q_0 | = | volume of injected source fluid |
| \dot{Q} | = | plume volumetric flow rate |
| \dot{Q}_0 | = | volumetric rate of injection of source fluid |
| Re_c | = | characteristic Reynolds number, $u_c l_u / \nu_\infty$ |
| Re_0 | = | source Reynolds number, $u_0 d / \nu_0$ |
| r | = | radial distance |
| t | = | time |
| t^* | = | self-preserving time scale |

| | | |
|------------------|---|---|
| u | = | vertical velocity |
| u_∞ | = | imposed crosstream velocity |
| $U(r/(x-x_0))$ | = | scaled variation of \bar{u} in the radial direction |
| v | = | radial velocity |
| $V(r/(x-x_0))$ | = | scaled variation of \bar{v} in the radial direction |
| w | = | tangential velocity |
| x | = | streamwise (vertical) distance |
| y | = | crosstream (horizontal) distance |
| ν | = | kinematic viscosity |
| ρ | = | density |
| Subscripts | | |
| c | = | centerline value |
| d | = | delay |
| max | = | maximum value |
| $stop$ | = | effective end of source flow |
| o | = | initial or virtual origin value |
| ∞ | = | ambient value |
| Superscripts | | |
| $(\bar{\quad})$ | = | time-averaged value |
| $(\bar{\quad})'$ | = | rms fluctuating value |

INTRODUCTION

Recent progress toward understanding and modeling the structure and penetration properties of round buoyant turbulent thermals, starting plumes and steady plumes (denoted thermals, starting plumes and steady plumes in the following) in still and crossflowing unstratified uniform environments is reviewed. These flows are of interest for several reasons: they have practical applications to interrupted, developing and steady nonreactive gas and liquid releases caused by process upsets, explosions and fires; they are simple classical flows that are relatively easy to interpret in order to better understand the

properties of steady and unsteady buoyant turbulent flows; and they involve uncomplicated geometries having well-defined initial and boundary conditions that provide measurements useful for evaluating models of practical buoyant turbulent flows. Study of these flows generally has been limited to conditions far from the source where analysis based on the self-preserving turbulent flow approximation has proven to be surprisingly successful. This approach has provided convenient ways to interpret and correlate the properties of relatively complex flows such as thermals, starting plumes and steady plumes in still and crossflowing environments. Motivated by these observations, the present review will consider the properties of these flows emphasizing self-preserving conditions.

The review begins with consideration of the structure properties of round buoyant turbulent flows, where past work has largely been limited to steady plumes in still environments so that measurements are reasonably tractable. Subsequent discussion of flow penetration properties will involve unsteady flows in both still and crossflowing unstratified uniform environments, considering the penetration properties of the following flow configurations: thermals in still environments, starting plumes in still environments, thermals in crossflows and starting plumes in crossflows. Discussion of the various flows can be read independently and each is organized as follows: introduction, experimental methods, theoretical methods, results and discussion, and conclusions. Detailed methods of modeling these flows have been addressed by others, see Baum et al.¹⁻³ and references cited therein; therefore, present considerations emphasize measurements and approximate analysis needed to find self-preserving scaling laws. Finally, several

reviews of early work concerning buoyant turbulent flows have appeared, see Turner,^{4,5} Tennekes and Lumley,⁶ Hinze,⁷ Chen and Rodi,⁸ List,⁹ and references cited therein; therefore, the present discussion emphasizes more recent studies.

STRUCTURE OF STEADY PLUMES IN STILL ENVIRONMENTS

Introduction

The structure of steady plumes in still environments is an important fundamental problem that has attracted significant attention since the classical study of Rouse et al.¹⁰ The earliest work of Rouse et al.,¹⁰ Morton et al.¹¹ and Morton¹² concentrated on the scaling of mean flow properties within fully-developed plumes, where flow properties become independent of source disturbances and source momentum and satisfy self-preserving scaling laws that provide simple correlations of appropriately normalized flow properties. Measurements of mean properties generally have satisfied the resulting scaling relationships, however, there are considerable differences among the various determinations of centerline property values, radial distributions of flow properties, and flow widths, see Refs. 8-27 and references cited therein. Aside from problems of experimental methods in a few instances, List⁹ and Papanicolaou and List^{22,23} attribute these differences to problems of reaching fully-developed, self-preserving, steady plume conditions.

One parameter that is helpful for estimating when steady plumes become self-preserving is the distance from the virtual origin normalized by the source diameter, $(x-x_0)/d$. This parameter is a measure of conditions where distributions of flow

properties appropriate for the often confined conditions of a source, have adjusted to reach distributions appropriate for an unconfined plume. The value of $(x-x_0)/d$ for self-preserving behavior depends on the nature of the flow, the properties of the source and the property of the flow for which self-preserving behavior is sought. For example, based on results for nonbuoyant round turbulent jets, values of $(x-x_0)/d$ greater than roughly 40 and 100 should be required to obtain self-preserving flow structure properties, based on distributions of mean and fluctuating (turbulent) properties, respectively.⁶ By these measures, the past measurements of plume structure of Refs. 10-25, which generally involved buoyant jets for the plume source, probably involve transitional plumes, e.g., they generally are limited to $(x-x_0)/d \leq 62$. The main reason for not reaching large values of $(x-x_0)/d$ for plumes, similar to jets, is that scalar properties decay much faster for plumes than for jets, e.g., proportional to $(x-x_0)^{-5/3}$ for plumes compared to $(x-x_0)^{-1}$ for jets.⁹⁻¹² Thus, an unusually large dynamic range for measuring scalar properties is required to maintain experimental uncertainties at a reasonable values far from the source within plumes. Contributing factors are that plume velocities are relatively small compared to jet velocities so that using velocity measurements to define self-preserving plume properties is also problematical and controlling room disturbances far from the source is more difficult for plumes than for jets due to the relatively small streamwise momentum levels of plumes.

A second parameter that is helpful for estimating when steady plumes become self preserving is the distance from the virtual origin normalized by the Morton length scale, $(x-x_0)/\ell_M$, as a measure of conditions where the momentum of the

plume resulting from effects of buoyancy is much larger than the momentum of the flow at its source. For general buoyant jet sources the Morton length scale is defined as follows:^{9,12,21}

$$\ell_M = \dot{M}_o^{3/4} / \dot{B}_o^{1/2} \quad (1)$$

For steady round plumes with uniform properties defined at the source (similar to the flows of interest in the following), the source specific momentum flux, \dot{M}_o , and the source specific buoyancy flux, \dot{B}_o , can be computed as follows:^{9,28}

$$\dot{M}_o = (\pi/4)d^2u_o^2 \quad (2)$$

$$\dot{B}_o = (\pi/4)d^2u_o g |\rho_o - \rho_\infty| / \rho_\infty \quad (3)$$

where an absolute value has been used for the density difference in Eq. (3) in order to account for both rising and falling plumes. Substituting Eqs. (2) and (3) into Eq. (1) then yields the following expression for the Morton length scale of steady round plumes having uniform source properties:

$$\ell_M/d = (\pi/4)^{1/4} (\rho_\infty u_o^2 / (g |\rho_o - \rho_\infty|))^{1/2} \quad (4)$$

The ratio, ℓ_M/d , is proportional to the source Froude number, which is defined as follows for conditions appropriate for the use of Eq. (4):⁹

$$Fr_o = (4/\pi)^{1/2} \ell_M/d = ((\rho_\infty u_o^2 / (g |\rho_o - \rho_\infty|))^{1/2}) \quad (5)$$

The source Froude number is a convenient measure of the dominance of buoyancy at the source, e.g., $Fr_o = 0$ and ∞ for purely buoyant and purely nonbuoyant sources, respectively. Thus, $(x-x_0)/\ell_M$, is a reasonable measure of conditions where

effects of source momentum have been lost and the momentum of the flow is dominated by effects of buoyancy. For example, purely buoyant sources have $Fr_o = \ell_M = 0$ and are immediately dominated by effects of buoyancy whereas purely nonbuoyant sources have $Fr_o = \ell_M = \infty$ and are never dominated by effects of buoyancy. Papanicolaou and List^{21,22} suggest that the buoyancy-dominated conditions for mean and fluctuating quantities in plumes are reached when $(x-x_o)/\ell_M$ is greater than roughly 6 and 14, respectively. A greater proportion of the measurements of mean properties of Refs. 10-27 exceed this criterion, however, the effects of transitional plume behavior (in terms of $(x-x_o)/d$) on these observations raises questions about the accuracy of these values of $(x-x_o)/\ell_M$ for the onset of self-preserving behavior for plumes.

A third criterion also should be satisfied when self-preserving conditions are reached; namely, that the density of the plume fluid should be linearly related to the degree of mixing of ambient and source fluid.³⁰ At self-preserving conditions in plumes, which generally are far removed from the complexities of practical sources such as fires, all scalar properties are conveniently represented by functions of the mixture fraction (which corresponds to the mass fraction of source material in a sample), called state relationships.²⁸⁻³⁰ Typically, the mixture fraction, $f \ll 1$, at self-preserving conditions so that the state relationship giving the density as a function of mixture fraction can be linearized as follows:²⁸⁻³⁰

$$\rho = \rho_\infty + f\rho_\infty(1 - \rho_\infty/\rho_o), \quad f \ll 1 \quad (6)$$

This provides a useful relationship for the driving potential for effects of buoyancy, as follows:

$$|d(\ln \rho)/df|_{f \rightarrow 0} = |\rho_o - \rho_\infty|/\rho_o \quad (7)$$

Virtually all the studies of Refs. 10-27, seeking to observe self-preserving steady plume properties, satisfy the $f \ll 1$ criterion required for a linear relationship between mixture fraction and density.

The preceding discussion suggests that the measurements of mean and fluctuating properties within plumes of Refs. 10-27, mainly involved transitional plumes combined with experimental difficulties in some instances.²⁸ Prompted by this observation, a series of studies were undertaken by Dai et al.,²⁸⁻³¹ seeking to better identify the conditions required to observe self-preserving round plumes in still and unstratified environments, and to determine the mean and turbulent structure of the flow at these conditions, including mixture-fraction, velocity and velocity/mixture-fraction statistics. These studies will be described in the following, considering experimental methods, theoretical methods, results and discussion, and conclusions, in turn. The following discussion is brief, see Dai et al.²⁸⁻³¹ for more details.

Experimental Methods

A sketch of the experimental apparatus for observations of steady round plumes in still and unstratified environments appears in Fig. 1. The test plumes were within a screened enclosure that was located in turn within an outer plastic enclosure. The screened enclosure could be traversed in order to accommodate rigidly mounted optical instrumentation. The plume sources were long round tubes having various

diameters, inlet flow straighteners and length-to-diameter ratios of 50:1. The sources could be traversed in the vertical direction to allow measurements at different streamwise positions. The source flows were either carbon dioxide or sulfur hexafluoride to provide negatively buoyant gaseous plumes that were exhausted from the test area using a dispersed exhaust system located at the floor. Source gas flows were controlled and measured using pressure regulators in conjunction with critical flow orifices. Mean and fluctuating mixture fraction properties were measured using laser-induced fluorescence (LIF) of iodine vapor seeded into the source flow. Seeding was done by passing a portion of the source flow through a bed of iodine crystals and then mixing this flow back into the main source flow. The LIF signal was produced by the unfocused beam of an argon-ion laser (at the 514.5 nm green line) which is absorbed by iodine and causes it to fluoresce at longer wavelengths in the visible yellow portion of the spectrum. The LIF signal was separated from scattered laser light using long-pass filters having 520 nm cut-off wavelengths. The detector outputs were sampled at constant time intervals and processed using a digital laboratory computer. Effects of preferential diffusion of iodine relative to carbon dioxide and sulfur hexafluoride were small; see Dai et al.²⁸ for additional details about monitoring and processing LIF signals and estimates of experimental uncertainties.

Mean and fluctuating velocity properties were measured using dual-beam, frequency-shifted laser velocimetry (LV), based on the 514.5 nm line of an argon-ion laser. The optical axis of the LV passed horizontally through the flow with signal collection at right angles to the optical axis. The beam plane was rotated in order to measure the streamwise and crosstream

components of velocity. The detector output was processed using a burst counter and the low pass-filtered analog output of the processor was sampled at equal time intervals in order to avoid velocity bias, whereas directional bias and ambiguity were controlled by frequency shifting. The source flow was seeded with oil drops with seeding levels controlled so that step noise contributed less than 3 percent to determinations of velocity fluctuations, see Dai et al.²⁹ for additional details about processing LV signals and experimental uncertainties. Finally, combined measurements of mixture fractions and velocities were undertaken using combined LIF/LV as described by see Dai et al.³⁰

Source conditions for the carbon dioxide and sulfur hexafluoride plumes were as follows: source diameters of 9.7 and 6.4 mm, mean velocities of 1.74 and 1.89 m/s, Reynolds numbers of 2000 and 4600, Froude numbers of 7.80 and 3.75, and values of ℓ_M/d of 7.34 and 3.53. Ambient air properties for these flows involved pressures and temperatures of 99 ± 0.5 kPa and 297 ± 0.5 K which implies an ambient density and kinematic viscosity of 1.16 kg/m³ and 14.8 mm²/s.

Theoretical Methods

Analysis has been undertaken to provide the self-preserving scaling laws for mean and fluctuating mixture fractions, velocities and combined mixture-fraction/velocity properties. A sketch of the steady plume arrangement considered appears in Fig. 2. The following assumptions were made about the flow: the flow is steady and axisymmetric in the mean, the source flow is known and is aligned with the gravitational vector, the ambient gas is known and is motionless and unstratified, the state relationship for density

is linear according to Eqs. (6) and (7) and satisfies the Boussinesq approximation (e.g., $|\rho - \rho_\infty|/\rho_\infty \ll 1$), the boundary layer approximations apply, Reynolds numbers are sufficiently large so that molecular transport can be neglected, and the flow is self-preserving. Under these assumptions, conservation principles and the state relationship for density imply that the buoyancy flux in the streamwise (vertical) direction is conserved for buoyant turbulent plumes.

Under the previous assumptions, mean mixture fractions and streamwise velocities can be scaled as follows in the self-preserving region, based on analyses due to Chen and Rodi,⁸ List,⁹ Rouse et al.,¹⁰ Morton et al.,¹¹ and Morton.¹²

$$\bar{f} g |d \ln \rho / df|_{r \rightarrow 0} (x - x_0)^{5/3} / \dot{B}_0^{2/3} = F(r/(x - x_0)) \quad (8)$$

$$\bar{u} ((x - x_0) / \dot{B}_0)^{1/3} = U(r/(x - x_0)) \quad (9)$$

where the virtual origin location of the source, x_0 , has been introduced in order to extend the region where self-preserving behavior is observed as much as possible toward the source. Notably, except for the virtual origin location, the only source properties appearing in Eqs. (8) and (9) are the plume buoyancy flux, \dot{B}_0 , and the source density, ρ_0 ; this behavior follows because the details of the source are not important in the self-preserving region, only the buoyancy flux, which is a conserved plume property, and ρ_0 which affects the driving potential for buoyancy effects. Finally, recalling Eq. (7), Eq. (8) can be rewritten to more directly indicate the roles of source and ambient density on flow mixing properties, as follows:

$$\bar{f} g |1 - \rho_\infty / \rho_0| (x - x_0)^{5/3} / \dot{B}_0^{2/3} = F(r/(x - x_0)) \quad (10)$$

Viewed in this form, Eqs. (9) and (10) clearly indicate that \dot{B}_0 and ρ_0 are the only relevant properties of the source in the self-preserving region of the plumes.

All other variables in the self-preserving region of plumes can be normalized in terms of the scaled variables of Eqs. (8)-(10), or equivalently in terms of \bar{f}_c and \bar{u}_c , which is typical of methods for reducing turbulence properties for self-preserving flows, see Tennekes and Lumley,⁶ Hinze,⁷ Chen and Rodi,⁸ List⁹ and references cited therein. Examples along these lines considered in the following include \bar{f}' / \bar{f}_c , $r \bar{v} / ((x - x_0) \bar{u}_c)$, \bar{u}' / \bar{u}_c , $\bar{f}' \bar{w}' / (\bar{f}_c \bar{u}_c)$, $\bar{f}' \bar{v}' / (\bar{f}_c \bar{u}_c)$ and $\bar{f}' \bar{u}' / (\bar{f}_c \bar{u}_c)$.

The functions $F(r/(x - x_0))$ and $U(r/(x - x_0))$ in Eqs. (8)-(10) are appropriately scaled radial distribution functions of mean mixture fractions and streamwise velocities, that are universal functions in the self-preserving region far from the source where Eqs. (8)-(10) apply. The radial distribution functions typically are approximated by Gaussian fits, as follows:⁸⁻¹⁰

$$F(r/(x - x_0)) = F(0) \exp\{-k_f^2 (r/(x - x_0))^2\} \quad (11)$$

$$U(r/(x - x_0)) = U(0) \exp\{-k_u^2 (r/(x - x_0))^2\} \quad (12)$$

where

$$k_f = (x - x_0) / \ell_f, \quad k_u = (x - x_0) / \ell_u \quad (13)$$

are constant plume width coefficients in the self-preserving region and ℓ_f and ℓ_u are characteristic plume radii where $\bar{f} / \bar{f}_c = \bar{u} / \bar{u}_c = \exp(-1)$, respectively.

Finally, defining a characteristic plume Reynolds number as follows:

$$\text{Re}_c = \ell_u \bar{u}_c / v_\infty \quad (14)$$

Then substituting for \bar{u}_c and ℓ_u in Eq. (14) from Eqs. (9) and (13), yields:

$$\text{Re}_c = U(0) (\dot{B}_0 (x-x_0)^2)^{1/3} / (k_u v_\infty) \quad (15)$$

Noting that $U(0)$ and k_u are universal constants, whereas \dot{B}_0 and v_∞ are constants for any given plume, Eq. (15) shows that the Reynolds numbers for self-preserving plumes progressively increase with increasing distance from the source, proportional to $(x-x_0)^{2/3}$, implying progressively larger ranges of length scales, and ratios of macro/micro scales of the turbulence, as the distance from the source increases.⁶

Results and Discussion

Measurements of steady plumes undertaken by Dai and coworkers,²⁸⁻³¹ in order to define conditions required to achieve self-preserving behavior and to find the properties of self-preserving plumes, will be considered in the following. A picture of the development of transitional plumes toward self-preserving conditions can be obtained from the radial distributions of mean mixture fractions for both carbon monoxide and sulfur hexafluoride source flows is illustrated in Fig. 3. In this case, the scaling parameters of Eq. (10) are used so that the ordinate is equal to $F(r/(x-x_0))$. The measurements are plotted for various streamwise distances with $(x-x_0)/d \geq 7$. The radial distributions of mean mixture fractions exhibit a progressive narrowing, with the value of $F(0)$ progressively increasing, with increasing distance from the source. Self-preserving conditions, where

the scaled mean mixture fraction distributions no longer vary with increasing streamwise distance, are observed when $(x-x_0)/d \geq 87$, which also corresponds to $(x-x_0)/\ell_M \geq 12$. This range of conditions also corresponds to characteristic plume Reynolds numbers of 2300-5900, which are reasonably large for unconfined turbulent flows,⁶⁻⁸ e.g., this range is comparable to the largest wake Reynolds numbers where measurements of round steady turbulent wakes have been reported, whereas turbulent wakes exhibit self-preserving turbulence properties at characteristic wake Reynolds numbers as small as 70.³² Within the self-preserving region, the radial distributions of mean mixture fractions were reasonably approximated by a Gaussian fit, as mentioned in connection with the discussion of Eq. (11); the parameters of this fit will be discussed later so that mean streamwise velocity properties can be considered at the same time. Finally, a surprising feature about the results of Fig. 3 is that reaching self-preserving conditions for mean quantities is significantly delayed beyond the region generally considered during past studies of the self-preserving properties of steady plumes, e.g., Refs. 10-25, and are also significantly delayed from conditions required for self-preserving mean properties within round nonbuoyant turbulent jets, $(x-x_0)/d = 40$, discussed by Tennekes and Lumley.⁶

The approach of steady plumes to self-preserving turbulence properties is illustrated in Fig. 4, where radial distributions of rms mixture fraction fluctuations (denoted mixture fraction fluctuations in the following) are plotted in terms of self-preserving variables at various streamwise distances from the source. Near the source, the distributions are rather broad and exhibit a dip near the axis, much like the behavior of nonbuoyant jets, see

Papanicolaou and List^{21,22} and Becker et al.³³ The mixture fraction fluctuation distributions evolve, however, with both the width and the magnitude of the dip near the axis gradually decreasing with increasing streamwise distance. Eventually, self-preserving conditions are reached for mixture fraction fluctuations at conditions similar to the self-preserving conditions for mean mixture fractions, e.g., $(x-x_0)/d \geq 87$ and $(x-x_0)/\ell_M \geq 12$. This behavior is comparable to conditions required for self-preserving turbulence properties in nonbuoyant jets, $(x-x_0)/d = 100$, discussed by Tennekes and Lumley.⁶ This result is also not surprising because self-preserving conditions for mean properties are generally a necessary condition for self-preserving conditions for fluctuating properties for turbulent flows.⁶ The gradual disappearance of the dip in mixture fraction fluctuations is an interesting feature of the results illustrated in Fig. 4. The development of the flow from source conditions where mixture fraction fluctuations are smaller than 1 percent is certainly a factor in this behavior. In addition, the presence of effects of turbulence production due to buoyancy, as $(x-x_0)/\ell_M$ increases, is also a factor. In particular, nonbuoyant jets have reduced mixture fraction fluctuations near the axis because turbulence production is small in this region due to symmetry requirements;^{21,22,33} in contrast, effects of buoyancy provide turbulence production near the axis of plumes in spite of symmetry due to buoyant instability in the streamwise direction, e.g., the density always approaches the ambient density in the streamwise direction.

The radial distributions of mean streamwise velocities in plumes within the self-preserving region, $(x-x_0)/d \geq 87$ and $(x-x_0)/\ell_M \geq 12$, are illustrated in Fig. 5. These

results are plotted according to the self-preserving variables of Eq. (9) so that the ordinate is equal to $U(r/(x-x_0))$. The variation of $U(r/(x-x_0))$ was reasonably approximated by a Gaussian fit, as mentioned in connection with the discussion of Eq. (12); the parameters of this fit will be discussed later.

Consideration of conservation of mass for round turbulent plumes satisfying the Boussinesq approximation shows that $r\bar{v}/((x-x_0)\bar{u}_c) = V(r/(x-x_0))$ where $V(r/(x-x_0))$ is a universal function for self-preserving plumes.²⁹ Mean radial velocities in plumes based on the measurements of Dai et al.²⁹ are plotted in Fig. 6 for self-preserving conditions, $(x-x_0)/d \geq 87$ and $(x-x_0)/\ell_M \geq 12$. These measurements are compared with results obtained indirectly from measurements of mean streamwise velocities through the conservation of mass expression. The results indicate good internal consistency of the measurements of mean streamwise and radial velocities because they agree with estimates obtained from measurements of mean streamwise velocities through the conservation of mass equation. In addition, the fact that $V(r/(x-x_0))$ is clearly universal for the range of the measurements illustrated in Fig. 6 supports the existence of self-preserving behavior for these conditions. These results also yield direct information about flow entrainment properties that play an important role in simplified integral theories of turbulent plumes, see Morton et al.¹¹ and Morton.¹² In particular:²⁹

$$d\dot{Q}/dx = (r\bar{v})_\infty = E_0 \ell_u \bar{u}_c \quad (17)$$

where E_0 is the entrainment coefficient of integral theories. Introducing the appropriate self-preserving plume properties

into Eq. (17) and solving for the entrainment coefficient then yields:

$$E_o = 5/(6 k_u) \quad (18)$$

The values of E_o found from the velocity measurements of Dai et al.²⁹ will also be discussed subsequently.

Radial distributions of streamwise velocity fluctuations measured in the self-preserving region of plumes by Dai et al.²⁹ are illustrated in Fig. 7. These results are plotted in terms of the self-preserving normalization of velocity fluctuations discussed earlier. Similar to the other plume variables, the streamwise velocity fluctuations are seen to properly satisfy the requirements for self-preserving behavior. In this case, the presence of the dip in streamwise velocity fluctuations near the axis seen in Fig. 7 is similar to behavior seen in nonbuoyant jets, see Ref. 22 and references cited therein. This behavior is expected due to reduced turbulence production near the axis due to symmetry without the presence of a supplemental mechanism for turbulence production that was observed for mixture fraction fluctuations near the axis.

Consideration of combined correlations involving mixture fraction and velocity fluctuations also support self-preserving behavior for the same range of conditions found for pure mixture fraction and velocity statistics. Evidence of this behavior is provided in Fig. 8, where radial distributions of turbulent mass fluxes are plotted according to the expectations of self-preserving behavior for $(x-x_o)/d \geq 87$ and $(x-x_o)/\ell_M \geq 12$. These results show that tangential turbulent mass fluxes are negligible as they should be for an axisymmetric flow, and that direct

determinations of radial tangential mass fluxes are internally consistent with measurements of streamwise tangential mass fluxes through the governing equation for conservation of mean mixture fractions. In addition, the measurements illustrated in Fig. 8 clearly agree with the expectations of self-preserving behavior. Finally, the contribution of the streamwise turbulent mass flux to the total streamwise mixture fraction transport is significant (roughly 15%) and must be considered for accurate determination of the buoyancy flux of the plume and for conservation checks, e.g., integral theory considerations of plumes based only on transport by mean quantities will yield errors on the order of 15% in the self-preserving portion of the flow due to effects of streamwise turbulent mass fluxes that are generally ignored for these theories.

Measurements of temporal power spectral densities of mixture fraction fluctuations of plumes were also reported by Dai et al.,²⁸ considering $(x-x_o)/d \geq 25$ and $r/(x-x_o)$ of 0.0-0.2. The spectra exhibited an initial decay according to the conventional $-5/3$ power of frequency,^{6,7} followed by a region where the decay was more rapid, according to the -3 power of frequency. The latter fast-decay region has been observed during several investigations of buoyant turbulent flows but has not been observed in nonbuoyant flows, see Papanicolaou and List.^{21,22} Notably, the spectra through the -3 decay region could all be plotted in a universal manner, based on self-preserving variables. An exception was that effects of progressively increasing Reynolds numbers with increasing distance from the source, see Eq. (15), naturally modified micro scales and thus the high-frequency portions of the spectra, which never can be self-preserving in plumes. The behavior of the low frequency portions of the spectra is notable as another example of

the fact that various flow properties reach self-preserving behavior at various distances from the source of the flow, and that some variables (e.g., temporal power spectra) exhibit self-preserving behavior quite close to the source. Other examples of behavior of this type will be found subsequently when the penetration properties of various types of round buoyant turbulent flows are considered.

The measurements of Dai et al.²⁸⁻³¹ generally were carried out farther from the source than earlier measurements of self-preserving plume properties and yield narrower distributions and larger values near the axis (when appropriately scaled) of flow properties than earlier results in the literature. This behavior is quantified in Table 1, where the medium of the flow (gas or liquid), the range of streamwise distances considered for measurements of the radial distributions of self-preserving plume properties, and the corresponding values of k_f^2 , $\ell_f/(x-x_0)$, $F(0)$, $(\bar{f}'/\bar{f})_c$, k_u^2 , $\ell_u/(x-x_0)$, $U(0)$, $(\bar{u}'/\bar{u})_c$ and E_0 are summarized by representative recent studies. Past measurements generally satisfy the criterion for buoyancy-dominated flow, i.e., $(x-x_0)/\ell_M > 6$, see Papanicolaou and List.^{21,22} Except for the measurements of Dai et al.,²⁸⁻³¹ however, the measurements summarized in Table 1 were obtained at values of $(x-x_0)/d$ that are not normally associated with self-preserving conditions for round turbulent buoyant jet sources. Similar to the tendency for transitional plumes to have broader radial distributions and smaller scaled values at the axis for \bar{f} and \bar{f}' than self-preserving plumes in Figs. 3 and 4, values of k_f^2 , $F(0)$ and $(\bar{f}'/\bar{f})_c$ all tend to decrease, whereas values of $\ell_f/(x-x_0)$ tend to increase, as the maximum streamwise values of $(x-x_0)/d$ of the measurements is decreased. This behavior yields a reduction

of the characteristic plume radius, and an increase of the scaled mean mixture fraction at the axis of 30 percent, when approaching self-preserving conditions over the range of maximum streamwise distances considered in Table 1. The behavior of streamwise velocities is similar, yielding a reduction of the characteristic plume radius of 40 percent, and an increase of the scaled mean streamwise velocity at the axis of 30 percent. Discrepancies between transitional and self-preserving plumes of this magnitude have a considerable impact on the empirical parameters obtained by fitting turbulence models to measurements. For example, Pivovarov et al.³⁴ suggest that the standard set of constants used in empirical turbulence models is inadequate based on the assumption of self-preserving plumes in conjunction with past measurements of transitional plumes, however, their predictions using standard constants are in reasonably good agreement with the measurements of self-preserving plume properties of Dai et al.,²⁸⁻³¹ that were just discussed, see Dai³⁵ for the details of this evaluation.

Conclusions

The properties of steady round turbulent buoyant plumes in still and unstratified environments were reviewed, yielding the following major conclusions:

1. Dai et al.²⁸⁻³¹ observed self-preserving behavior for all plume properties for $(x-x_0)/d \geq 87$ and $(x-x_0)/\ell_M \geq 12$, which is significantly farther from the source than earlier measurements of self-preserving plume properties that were limited to $(x-x_0)/d \leq 62$.¹⁰⁻²⁵ Within the self-preserving region, observations of mean properties of plumes due to Dai et al.²⁸⁻³¹ yielded plume widths that were 30-40 percent narrower, with scaled mean values at the axis 30

percent larger, than the earlier observations of Refs. 10-25.

2. Differences of the properties of plumes of the magnitude just mentioned, due to failure to achieve self-preserving conditions, can have a considerable effect on the properties of approximate models of buoyant turbulent flows. For example, evaluation of turbulence models of steady self-preserving plumes due to Pivovarov et al.³⁴ found considerable deficiencies of conventional model constants using the measurements from Refs. 10-25, whereas similar evaluations due to Dai³⁵ found good performance of conventional model constants using the measurements from Dai et al.²⁸⁻³¹ In view of these observations, past evaluations of models of buoyant turbulent flows, based on the assumption of self-preserving flows within buoyant turbulent plumes using the measurements of Refs. 10-25, should be reconsidered.

3. Achieving self-preserving behavior for buoyant turbulent flows is affected by the nature of the flow, the properties of the source and the flow property considered. For example, Dai et al.²⁸⁻³¹ found that the low-frequency portions of temporal power spectra were self-preserving for $(x-x_0)/d$ as small as 25 (the smallest value that they considered) whereas self-preserving behavior for all properties of these flows was not observed until $(x-x_0)/d \geq 87$, as noted earlier.

4. Streamwise turbulent mass fluxes are quite large near the axis of steady plumes where corresponding mixture-fraction/velocity fluctuation correlation coefficients reach values of roughly 0.7. This behavior is responsible for the large turbulent mass flux contribution to the total streamwise buoyancy flux in plumes (roughly 15 percent). This contribution is

often ignored and leads to errors of flow properties estimated using integral models; it also leads to errors of conservation of buoyancy flux checks for other models of plumes.

PENETRATION OF THERMALS IN STILL ENVIRONMENTS

Introduction

The penetration properties of thermals in still environments is an important fundamental problem relevant to the dispersion of heat and harmful substances due to accidental releases caused by process upsets, explosions and fires. Due to measurement problems resulting from the unsteadiness of thermals, however, they have received considerably less attention than steady plumes. The few past investigations of round buoyant turbulent thermals in still and unstratified environments (denoted simply as thermals in the following) and related flows include studies reported by Scorer,³⁶ Turner,^{4,37} Richards,³⁸ Fay and Lewis,³⁹ Batt et al.⁴⁰ Thompson et al.,⁴¹ Turner,⁴² Morton,⁴³ and references cited therein. These studies have provided the self-preserving scaling rules that describe the penetration properties of thermals, e.g., the maximum vertical and radial penetration distances of the flows into the surroundings as a function of time. Corresponding measurements of the self-preserving properties of thermals, however, are surprisingly limited and involve concerns about whether self-preserving conditions were actually achieved.

Prompted by these observations, Sangras et al.⁴⁴ and Diez et al.⁴⁵ undertook closely related experimental studies of puffs (as the nonbuoyant limiting condition of a thermal) and thermals in still and

unstratified environments, seeking to determine the conditions required for self-preserving behavior and the vertical and radial penetration properties of the flows at self-preserving conditions, and to use the measured penetration properties to evaluate self-preserving scaling and to find the empirical factors needed to correlate the penetration properties of these flows. These studies will be described in the following, emphasizing thermals, and considering experimental methods, theoretical methods, results and discussion, and conclusions, in turn. The following discussion is brief, see Sangras et al.⁴⁴ and Diez et al.⁴⁵ for more details.

Experimental Methods

The experiments involved salt-water modeling of buoyant turbulent flows as suggested by Steckler et al.⁴⁶ A sketch of the test apparatus appears in Fig. 9. The apparatus consisted of a plexiglass water bath with source fluid injection at the top. The dense salt-containing source liquid settled naturally to the bottom of the tank and was removed from time-to-time using the water bath drain. The source fluid for the thermals was injected into the tank using smooth round glass tubes having length/diameter ratios greater than 50 to help insure fully-developed turbulent pipe flow for sufficiently large injector Reynolds numbers.⁴⁷ The source liquid was supplied to the injectors using syringe pumps that were computer controlled to start, stop and deliver liquid at preselected times and rates. Calibration of pump performance indicated nearly constant delivery rates with relatively short start and stop transients.⁴⁴ Salt-water source liquids were prepared by adding highly purified salt to given weights of water to reach desired source liquid densities. The densities of the present test fluids agreed with the tabulation of Lange⁴⁸

based on density measurements using precision hygrometers. A Cannon/Fenske viscometer was used to measure liquid viscosity. Finally, red vegetable dye was added to the source liquid in order to facilitate flow visualization of self-preserving behavior

Thermal penetration properties were measured as a function of time using video records of the flow. These records were obtained from observations through the side walls of the water bath after illuminating the dye-containing thermals with quartz lamps.

Test conditions can be summarized as follows: source diameters of 3.2 and 6.4 mm, source densities of 1071 and 1148 kg/m³, ambient densities of 998 kg/m³, source Reynolds numbers of 6000-12000, source Froude numbers of 10-82, and amounts of source fluid discharged, $Q_0/(A_0d)$, of 50-382.

Theoretical Methods

Assuming that the flow is in the self-preserving regime, expressions for the vertical flow penetration distance for thermals in still environments are available from Turner,^{4,5} List,⁹ Morton et al.,¹¹ Scorer,³⁶ Turner,³⁷ Richards,³⁸ and references cited therein. The configuration considered for thermals is illustrated in Fig. 10. The source flow enters from a passage having a diameter, d , with a density, ρ_0 , into an environment having a density, ρ_∞ ; properties of interest include the maximum vertical and radial penetration distances, x_p and r_p , illustrated on the figure. Major assumptions for analysis to find self-preserving flow scaling due to List,⁹ are as follows: physical property variations are small (i.e., the flows are weakly buoyant so that density variations are linear functions of the degree of mixing as discussed earlier),

sources are assumed to start and stop instantly and to maintain constant flow rates when the source fluid is flowing (extrapolated temporal origins or terminations were used to handle actual start and stop processes for measurements considered in the following), virtual origins were used to maximize conditions where self-preserving behavior is observed, and source flow properties are assumed to be uniform so that Eqs. (4) and (5) can be used to find ℓ_M/d and Fr_o .

Under these assumptions, the temporal variation of maximum vertical penetration distance can be expressed as follows within the self-preserving region of thermals:

$$(x_p - x_o)/d = C_x((t - t_d)/t^*)^n \quad (19)$$

where t_d is the extrapolated virtual origin to treat initiation of pump flow to the source, and the time of flow required to create the source is assumed to be small compared to values of $(t - t_d)$ of interest. The corresponding temporal variation of the maximum radial penetration distance can be expressed most conveniently in terms of the vertical penetration distance, as follows:

$$r_p/(x_p - x_o) = C_r \quad (20)$$

The same general form can be applied to a variety of round transient flows in still fluids — puffs, thermals, starting jets, starting plumes, etc. — with values of C_x , C_r , t^* and n varying depending upon the particular flow that is being considered. The values of C_x and C_r are best-fit empirical parameters of the self-preserving analysis and will be considered later when the measurements are discussed. The values of t^* and n , however, follow from the requirements for self-preserving flow and can be expressed as follows for round thermals:⁹

$$t^* = (d^4/B_o)^{1/2}, \quad n=1/2; \text{ thermal} \quad (21)$$

where B_o is the source specific buoyant force in the thermal defined by List.⁹ Under the present assumption of uniform source properties, the value of B_o for a thermal can be found from source properties, as follows:⁹

$$B_o = Q_o g |\rho_o - \rho_\infty| / \rho_\infty; \text{ thermal} \quad (22)$$

where the absolute value has been used for the density difference, as before, to account for both rising and falling flows.

The expressions for vertical penetration distance of thermals in still environments, Eqs. (19), (21) and (22), are convenient for illustrating the development of thermals toward self-preserving behavior, and their subsequent penetration properties in the self-preserving portion of the flow. This formulation is misleading, however, because it involves the source diameter which is not a relevant variable of self-preserving plumes. This is apparent because d cancels out of Eqs. (19) and (21), to yield the following expression for the vertical penetration distance of a self-preserving thermal in a still environment:

$$(x_p - x_o)/(B_o^{1/2} (t - t_d))^{1/2} = C_x; \text{ thermal} \quad (23)$$

where the theoretical value, $n = 1/2$, for self-preserving thermals has been used in Eq. (23).

Results and Discussion

Normalized vertical penetration distances for thermals are plotted according to the self-preserving scaling of Eqs. (19) and (21) in Fig. 11. The measurements agree reasonably well with self-preserving scaling for thermals for $(t - t_d)/t^* > 40$ and

$(x_p - x_o)/d > 40$, which also implies $(x_p - x_o)/\ell_M > 5$; in particular, the value of $n = 1/2$ for thermals is reasonably well confirmed by the measurements illustrated in Fig. 11.

Normalized maximum radial penetration distances for thermals are also plotted according to the self-preserving scaling of Eq. (20) in Fig. 12. More near-source points are plotted for the radial penetration results of Fig. 12 than are shown for the streamwise penetration results of Fig. 11; these points are omitted from Fig. 11 in order to reduce overlap of data points and improve clarity. The flow tends to approach self-preserving behavior for the radial penetration distance, where $r/(x_p - x_o) = C_r$ is a constant, when $(x_p - x_o)/d > 40$ which is similar to observations of streamwise penetration distances. The final value for the self-preserving region of thermals is $C_r = 0.19$, which is significantly larger than flow radii observed for steady plumes. Somewhat similar behavior was observed by Sangras et al.⁴⁴ for nonbuoyant starting jets and puffs where $C_r = 0.18$ and 0.16 , respectively. This effect appears to be due to motion of the ambient flow around the periphery of the thermal causing the thermal to flatten somewhat similar to the behavior of drops prior to secondary breakup, see Faeth.⁵⁰ This occurs because the flow along the axis tends to stagnate, raising its static pressure, whereas the flow near the periphery must spread out and this increases its velocity, lowering its pressure and deforming the thermal accordingly. In addition, measurements plotted according to the normalized expression for the vertical penetration distance from Eq. (23) are illustrated in Fig. 12; as already noted, the vertical penetration of thermals reaches self-preserving behavior at streamwise positions comparable to self-preserving radial

penetration, e.g., at $(x_p - x_o)/d > 40$, yielding $C_x = 2.10$.

A summary of the values of n , C_x and C_r is provided in Table 2, based on the measurements of Diez et al.,⁴⁵ Scorer,³⁶ Turner,³⁷ and Thompson et al.,⁴¹ for round turbulent thermals. These studies generally agree that the streamwise penetration is proportional to the time after the start of the flow to the $1/2$ power, however, the values of C_r are smaller for the results of Diez et al.⁴⁵ than the rest. Recalling that values of $r/(x_p - x_o) = C_r$ progressively decrease as $(x_p - x_o)/d$ increases until the self-preserving region is reached, where this parameter becomes constant, see Fig. 12, it is likely that the discrepancy occurs because the measurements were not obtained far enough from the source in Refs. 36, 37 and 41 for the self-preserving region to be reached.

Finally, the location of the virtual origin for thermals was studied by Diez et al.,⁴⁵ considering variations of the amount of source fluid in the plume in the range $Q_o/(A_o d) = 50-382$. Experimental uncertainties for x_o/d are relatively large because this variable depends on the slope of the streamwise penetration plot of $(x - x_o)/d$ as a function of dimensionless time, see Fig. 12. These results yielded $x_o/d = 9.0$ over this test range, which is a constant within experimental uncertainties.

Conclusions

The properties of unsteady round turbulent buoyant thermals in still and unstratified environments were reviewed, yielding the following major conclusions mainly based on the observations of Diez et al.⁴⁵

1. The flows became turbulent within 5 diameters from the source exit; although

near-source behavior varied significantly with source properties, self-preserving behavior generally was observed for $(x_p - x_o)/d > 40$ and $(x_p - x_o)/\ell_M > 5$.

2. Within the self-preserving region, the vertical dimensionless penetration distance, $(x_p - x_o)/d$, generally varied as a function of time in agreement with anticipated behavior for self-preserving thermals with maximum vertical penetration distance varying according to dimensionless time to the 1/2 power.

3. Within the self-preserving region, the normalized maximum radius of the flow grew as a function of time in the same manner as the normalized streamwise penetration distance, yielding $r_p/(x_p - x_o) = 0.19$.

4. The virtual origin of the flow was independent of the amount of source fluid used for the range considered during the experiments, e.g., x_o/d was equal to 9.0 for $Q_o/(A_o d)$ as large as 382. This behavior differs from nonbuoyant puffs, where x_o/d was observed to increase when $Q_o/(A_o d) > 120$. These differences appear to result from effects of buoyancy that isolate the thermal from the source, which is a mechanism that is not present for nonbuoyant flows.

PENETRATION OF STARTING PLUMES IN STILL ENVIRONMENTS

Introduction

The penetration properties of starting plumes in still environments is an important fundamental problem relevant to the unconfined and unsteady turbulent flows resulting from fluid releases caused by process upsets, explosions and unwanted fires. Due to its simplicity, this flow is also

of interest as a classical turbulent buoyant flow that helps illustrate the development of unsteady turbulent buoyant flows. Finally, due to well-defined initial and boundary conditions, the starting plume is useful for providing data needed to evaluate methods for predicting the properties of turbulent buoyant flows, particularly at self-preserving conditions where detailed definition of source properties is no longer needed. Similar to thermals, however, starting plumes have received less attention than steady plumes due to the measurement problems of unsteady flows. The few past investigations of round turbulent starting plumes in still and unstratified environments (denoted simply as starting plumes in the following) include studies reported by Turner,⁴⁹ Middleton,⁵¹ Delichatsios,⁵² Pantzloff and Lueptow,⁵³ and references cited therein. Similar to past investigations of thermals, these studies have provided self-preserving scaling rules that describe the main features of turbulent buoyant starting plumes, however, corresponding measurements of the self-preserving properties of these flows are surprisingly limited and involve concerns about whether self-preserving conditions were actually achieved.

Prompted by these observations, Diez et al.⁴⁵ undertook a study of starting plumes in still and unstratified environments using methods similar to Sangras et al.⁴⁴ The objectives were to determine conditions required for self-preserving behavior, to find the vertical and radial penetration properties of the flows at self-preserving conditions, and to use the measured penetration properties of these flows to evaluate self-preserving scaling and to find empirical factors needed to correlate the penetration properties of these flows. This study will be described in the following, considering experimental methods, theoretical methods,

results and discussion and conclusions, in turn. The following discussion is brief, see Diez et al.⁴⁵ for more details.

Experimental Methods

The experiments used the same apparatus as the study of thermals and the details of the measurements were the same.⁴⁵ The only change was that the source flow was maintained throughout the time period where measurements were made, in order to simulate starting plumes as opposed to thermals which involve interrupted source flows.

The test conditions for the starting plume studies can be summarized as follows: source diameters of 3.2 and 6.4 mm, source densities of 1071 and 1198 kg/m³, ambient densities of 998 kg/m³, source Reynolds numbers of 6000-12000, and source Froude numbers of 10-82.

Theoretical Methods

Assuming that the flow is in the self-preserving regime, expressions for the streamwise flow penetration distance for starting plumes are available from Turner,^{4,5,49} List,⁹ Middleton,⁵¹ Delichatsios,⁵² Pantzlauff and Lueptow,⁵³ and references cited therein. The configuration they considered for starting plumes is illustrated in Fig. 13. The source flow enters from a passage having a diameter, d , with a density, ρ_o , and flows into an environment having a density, ρ_∞ ; properties of interest include the maximum vertical and radial penetration distances, x_p and r_p , illustrated on the figure. Major assumptions for the starting plumes are similar to those used for thermals, as follows: physical property variations are small so that density is a linear function of the degree of mixing,

the source starts instantly and maintains a constant volumetric flow rate thereafter, a virtual origin is used to maximize conditions where self-preserving behavior is observed, and source flow properties are uniform so that Eqs. (4) and (5) can be used to find ℓ_M/d and Fr_o .

Under these assumptions, the temporal variation of the maximum streamwise penetration distance is given by Eq. (19) and the corresponding temporal variation of the maximum radial penetration distance is given by Eq. (20). The values of t^* and n , however, differ from the values for thermals, and are given as follows for round starting plumes:⁹

$$t^* = (d^4/\dot{B}_o)^{1/3}, \quad n = 3/4; \quad \text{starting plume} \quad (24)$$

where \dot{B}_o is the source specific buoyant flux in the plume. Under present assumptions of uniform source properties, the source specific buoyant flux for a plume can be found from source properties, as follows:⁹

$$\dot{B}_o = \dot{Q}_o g|\rho_o - \rho_\infty|/\rho_\infty; \quad \text{starting plume} \quad (25)$$

where an absolute value has been used for the density difference, as before, to account for both rising and falling plumes. The analogous formulation for nonbuoyant starting jets can be found in Sangras et al.⁴⁴

Similar to the earlier discussion about the presence of d in expressions for the self-preserving vertical penetration of starting plumes in still environments, Eqs. (19) and (24) can be rearranged to yield the following expression for the vertical penetration distance of a self-preserving starting plume in a still environment:

$$(x_p - x_0) / (\dot{B}_0^{1/3} (t - t_d))^{3/4} = C_x; \text{ starting plume} \quad (26)$$

where the theoretical value, $n = 3/4$, for self-preserving starting plumes has been used in Eq. (26).

Results and Discussion

The normalized vertical penetration distances of starting plumes are plotted according to the self-preserving scaling of Eqs. (19) and (24) in Fig. 14. Near-source behaviors vary depending upon source properties, however, present flows generally correspond to over-accelerated flows ($Fr_0 > 5$) so that the flows generally decelerate at first before self-preserving conditions are approached. All the measurements are seen to follow the self-preserving scaling at large dimensionless times, e.g., at $(t - t_d)/t^* > 20$ which corresponds to $(x_p - x_0)/d > 40$ and $(x_p - x_0)/\ell_M > 5$. Both these distances are much nearer to the source than the values of $(x - x_0)/d > 80$ and $(x - x_0)/\ell_M > 10$ needed to reach self-preserving behavior for round turbulent buoyant plumes based on measured mean and fluctuating mixture fraction and velocity distributions discussed in connection with Figs. 3-8. This observation highlights the fact that conditions for self-preserving behavior depend on the flow and on the property observed whereas radial flow widths tend to reach self-preserving behavior slower than other properties of most flows.

Normalized maximum radial penetration distances (found near the jet tip) of starting plumes are plotted according to the self-preserving scaling of Eq. (20) in Fig. 15. More near-source points are plotted in Fig. 15 than in Fig. 14 because some test conditions were omitted in Fig. 14 in order to reduce overlap and improve clarity of this figure. The normalized maximum radial

penetration distance has relatively large values in the region nearest the source where measurements were made; this is expected, however, because this property becomes unbounded at the virtual origin. The normalized maximum radial penetration distance decreases with increasing streamwise distance and becomes relatively constant in the self-preserving region where $(x_p - x_0)/d \geq 40$. As just noted, this radial flow parameter approaches self-preserving behavior at comparable conditions to streamwise penetration distance considered in Fig. 14. For self-preserving conditions, $r_p/(x_p - x_0) = C_r = 0.15$ which is smaller than the value of $C_r = 0.19$ for thermals as discussed in the section on thermals. In addition, measurements plotted according to the normalized expression for the vertical penetration distance from Eq. (26) are illustrated in Fig. 15; as already noted, the vertical penetration for starting plumes reaches self-preserving behavior at distances comparable to the radial penetration, e.g., at $(x_p - x_0)/d > 40$.

A summary of the values of n , C_x and C_r for starting plumes is provided in Table 3 considering the measurements of Diez et al.⁴⁵ and Turner.⁴⁹ The results for n for both studies agree with the expectations of self-preserving theory. The values of C_r are somewhat smaller for the measurements of Diez et al.⁴⁵ than for the measurements of Turner.⁴⁹ Based on the results of Fig. 15 it seems likely that this discrepancy occurs because the measurements of Diez et al.⁴⁵ were carried out farther from the source than those of Turner.⁴⁹

Conclusions

The properties of round turbulent buoyant starting plumes in still and unstratified environments were reviewed, yielding the following major conclusions,

mainly based on the observations of Diez et al.⁴⁵

1. The flows became turbulent within 5 diameters of the source exit; although near-source behavior varied significantly with source properties, self-preserving behavior generally was observed for $(x_p - x_0)/d \geq 40$ and $(x_p - x_0)/\ell_M \geq 5$.

2. Within the self-preserving region, the vertical dimensionless penetration distance, $(x_p - x_0)/d$, generally varied as a function of time in agreement with anticipated behavior for self-preserving starting plumes with maximum vertical penetration distances varying according to dimensionless time to the 3/4 power.

3. Within the self-preserving region, the normalized maximum radius of the flow grew as a function of time in the same manner as the normalized streamwise penetration distance, yielding $C_r = r_p/(x_p - x_0) = 0.15$, which is smaller than the earlier measurements of Turner⁴⁹ probably because the latter results were not obtained sufficiently far from the source to reach self-preserving conditions.

4. The value of C_r for starting plumes is smaller than the value found for thermals, $C_r = 0.15$ and opposed to 0.19, because the motion of the thermal tends to cause it to flatten in much the same way that drops are flattened as they move through an ambient gas environment.

PENETRATION OF THERMALS IN CROSSFLOWS

Introduction

The penetration properties of thermals in crossflowing environments is an

important fundamental problem relevant to the dispersion of heat and harmful substances due to accidental releases because crossflows are generally more prevalent than still environments during such releases. The additional complexities of providing well-defined crossflows has resulted in fewer studies of thermals in crossflows than in still environments. Some examples of early studies in this area include Andreopoulos,⁵⁵ Alton et al.,⁵⁶ Baum et al.,¹⁻³ Hasselbrink and Mungal,⁵⁷ and references cited therein. Similar to earlier studies of buoyant turbulent thermals and plumes, however, there are concerns about whether observations were carried out far enough from the source for self-preserving conditions to be reached. In addition available measurements of these flows are very limited due to problems of dealing with the transient and fundamentally three-dimensional nature of thermals in crossflows.

Prompted by these observations, Diez et al.⁵⁴ undertook measurements of thermals in uniform and unstratified crossflows, seeking to determine the conditions required for self-preserving behavior and the vertical, crosstream (horizontal) and radial penetration properties of the flows at self-preserving conditions, and to use the measured penetration properties to evaluate self-preserving scaling and to find empirical factors needed to correlate the penetration properties of this flow. The study of Diez et al.⁵⁴ will be emphasized in the following, considering experimental methods, theoretical methods, results and discussion, and conclusions, in turn. The following discussion is brief, see Diez et al.⁵⁴ for more details.

Experimental Methods

The experiments of Diez et al.⁵⁴ involved salt-water modeling of buoyant turbulent flows as suggested by Steckler et al.⁴⁶ similar to the studies of buoyant flows in still environments that were just discussed. A sketch of the test apparatus appears in Fig. 16. These experiments were carried out in a water channel facility with a test section having a 610×610 mm cross section and a streamwise length of 2000 mm. The water channel was a closed loop arrangement with water entering the plexiglass test section through a calming section, a flow straightener grid, a series of screens and a 10:1 contraction to provide a small turbulence intensity (< 1%) mean flow through the test section. The dense salt-containing source liquid settled naturally to the bottom of the water channel facility and was removed from time to time using the facility drain. The source fluid was the same as for the earlier studies of puffs, thermals and starting plumes in still environments due to Sangras et al.⁴⁴ and Diez et al.⁴⁵ The source fluid injection system was injected into the water channel using smooth glass tubes having length/diameter ratios greater than 50 to help insure fully-developed turbulent pipe flow at the tube exit for sufficiently large Reynolds numbers.⁴⁷ The source liquid was supplied to the injectors using syringe pumps that were computer-controlled to start, stop and deliver liquid at prescribed rates. The source liquid contained dye and was illuminated and photographed using color video cameras. The thermals were viewed through the sides and bottom of the water channel to provide measurements of maximum vertical, crossstream and radial penetration distances of the flow as a function of time.

Test conditions were as follows: source diameters of 3.2 and 6.4 mm, source densities of 1071 and 1148 kg/m³, ambient density of 998 kg/m³, source Reynolds numbers of 4,000-11,000, source Froude numbers of 14-82, amounts of source fluid discharged, $Q_0/(A_0 d)$ of 16-318, and ratios of source/cross-stream flow velocities of 5-35.

Theoretical Methods

Two key assumptions were made by Diez et al.⁵⁴ to treat thermals in uniform crossflows, both of which were motivated by the treatment of steady plumes in uniform crossflows due to Baum et al.,¹ namely: (1) the crossflow motion was assumed to involve uniform crossflows having negligible slip, and (2) the vertical motion was assumed to be equivalent to the vertical motion of a thermal in a uniform still environment, e.g., the crossflow was assumed to have a negligible impact on the vertical motion of the thermal. Rather than numerically compute the vertical motion of the flow similar to Baum et al.,¹ however, the temporal scaling of thermals in still environments was used to treat the vertical motion of the thermals in crossflow.

Assuming that the flow in the vertical direction is self-preserving, expressions for the vertical penetration of the thermals are available from Turner,^{4,5} List,⁹ Morton et al.,¹¹ Scorer,³⁶ Turner,³⁷ Richards,³⁸ and references cited therein. The configuration used by Diez et al.⁵⁴ for thermals in crossflow is illustrated in Fig. 17. The source flow enters from a passage having a diameter, d , with a density, ρ_0 , and velocity u_0 , and flows into an environment having a density, ρ_∞ , and a uniform crossflow velocity of u_∞ ; properties of interest include the maximum vertical, crossflow and radial penetration distances,

x_p , y_p and r_p , illustrated in Fig. 17. Major assumptions are similar to Baum et al.¹ in the crossflow direction and List⁹ in the vertical direction, as follows: physical property variations are small (i.e., the flows are weakly buoyant so that density variations are linear functions of the degree of mixing as discussed earlier for thermals in still environments), sources are assumed to start and stop instantly and to maintain constant flow rates when the source fluid is flowing (using extrapolated temporal origins or terminations to handle actual start and stop processes as before), virtual origins are used in both the vertical and crosstream directions to maximize conditions where self-preserving behavior is observed, crosstream motion is assumed to satisfy of the no-slip convection approximation whereas vertical motion is assumed to satisfy the same self-preserving relationships as thermals in still environments, and source flow properties are assumed to be uniform so that Eqs. (4) and (5) can be used to find ℓ_M/d and Fr_0 .

Under these assumptions, the temporal variation of the vertical penetration distance is given by Eq. (19), the corresponding temporal variation of the maximum radial penetration distance is given by Eq. (20), and the expressions for t^* , n and B_0 are the same as for thermals in still environments and are given by Eqs. (21) and (22) whereas Eq. (23) provides an analogous expression for the vertical penetration distance that does not involve d , which is not a relevant parameter at self-preserving conditions. The maximum crosstream penetration distance follows from the no-slip convection approximation, as follows:

$$(y_p - y_0)/d = C_y(u_\infty(t - t_d)/d) \quad (27)$$

The values of C_x and C_r in Eqs. (19) and (20) are best-fit empirical parameters that are expected to be similar to earlier results for self-preserving thermals based on the present approximations. The value of C_y in Eq. (27) is another best-fit empirical parameter that should be on the order of magnitude of unity if the no-slip convection approximation is valid for the crosstream direction. Finally, the various time delay parameters and the virtual origins in the vertical and crosstream directions are also best-fit empirical parameters that are expected to be functions of the amount of source fluid injected, similar to the earlier results concerning x_0 for thermals in still environments.

Results and Discussion

The crosstream (horizontal) penetration distances of thermals in uniform crossflows are plotted according to the no-slip convection approximation of Eq. (27) in Fig. 18. The results indicate that the no-slip convection approximation is satisfied for the range of measurements, which extends from horizontal displacements near zero, implying a virtual origin of the flow for this direction of essentially zero.

The vertical penetration distances of thermals in uniform crossflows are plotted according to the self-preserving scaling of Eqs. (19), (21) and (27) in Figs. 19 and 20. The measurements indicate that self-preserving scaling of thermals in crossflow occurs for $(t - t_d)(B_0/d^4)^{1/2} \geq 3000$, and $(x_p - x_0)/d \geq 80$. Within the self-preserving region the temporal rate of vertical penetration of thermals in crossflow proceeds according to $n=1/2$, similar to thermals in still environments.

Normalized maximum radial penetration distances of thermals in

crossflow are plotted according to the self-preserving scaling of Eq. (20) in Fig. 21 in terms of the dimensionless vertical penetration distance. In this case, the self-preserving condition is reached relatively similar to streamwise penetration, e.g., for $(x_p - x_o)/d > 80$, with $C_r = 0.14$, which is appreciably smaller than the value of $C_r = 0.19$ for thermals in still environments. These last observations are somewhat surprising because most other features of thermals in still and uniform crossflowing environments are similar. In addition, measurements plotted according to the normalized expression for the vertical penetration distance from Eq. (23) are illustrated in Fig. 21; as already noted, vertical penetration for thermals in crossflow reaches self-preserving behavior comparable to radial penetration, e.g., at $(x_p - x_o)/d > 80$.

The location of the virtual origin of thermals in uniform crossflow was studied by Diez et al.,⁵⁴ considering variations of the amount of source fluid in the range 18-318. It was found that the virtual origin was essentially independent of the amount of source fluid used in this range, with $x_o/d = -20$, which is very similar to the value found for thermals in still environments.

Finally, the various properties of thermals in crossflow are summarized in Table 4. Most of the properties of thermals in still environments (see Table 2) and in crossflow are similar except for C_r as just noted.

Conclusions

The properties of unsteady round turbulent buoyant thermals in uniform and unstratified crossflow were reviewed yielding the following major conclusions,

mainly based on the observations of Diez et al.⁵⁴

1. The flows became turbulent within 5 diameters from the source exit; although near source behavior varied significantly with source properties, self-preserving behavior generally was observed for $(x_p - x_o)/d \geq 80$ and $(x_p - x_o)/\ell_M > 10$.
2. Within the self-preserving region, vertical dimensionless penetration distances generally varied as a function of time in accord with behavior expected for self-preserving thermals, e.g., varying according to dimensionless time to the 1/2 power.
3. Throughout the entire temporal range of observations, the no-slip crossstream convection approximation for thermals in uniform crossflow was satisfactory, yielding a simple and convenient way of estimating flow trajectories.
4. Radial penetration distances for thermals in uniform crossflow also satisfied the general scaling relationships observed for thermals in still environments. The value of $C_r = 0.14$ for thermals in crossflow is significantly smaller than the value of 0.19 observed for thermals in still environments for reasons that have not been resolved.
5. The virtual origins of thermals in both crossflow and in still fluids were independent of the amount of source fluid used for $Q_o/(A_o d) < 312$ with y_o/d of -20 and -23 , respectively.

PENETRATION OF STARTING PLUMES IN CROSSFLOW

Introduction

The penetration properties of starting plumes in crossflowing environments is an important fundamental problem relevant to the dispersion of heat and harmful substances due to accidental releases because releases are generally of extended duration so that the starting thermal approaches self-preserving starting plume behavior whereas releases occur in the presence of significant crossflow more often than not. Similar to the other unsteady flows already considered, however, starting plumes in crossflow have not been measured very often due to the complexities of providing well-defined crossflows and the difficulties of measuring the properties of three-dimensional unsteady flows. Some examples of past studies in this area include Baum et al.,¹⁻³ Andreopoulos,⁵⁵ Alton et al.,⁵⁶ Hasselbrink and Mungal,⁵⁷ and references cited therein. Similar to the other flows discussed in this review, the measurements of Refs. 55-57 are limited and there are concerns about whether these experiments were carried out far enough from the source for self-preserving conditions to be reached.

Prompted by these observations, new measurements of the properties of starting plumes in uniform and unstratified crossflow are currently in progress in this laboratory, in order to gain a better understanding of the self-preserving behavior of these flows. Initial results from this study will be discussed in the following, considering experimental methods, theoretical methods, results and discussion, and conclusions, in turn.

Experimental Methods

The experiments used the same water tunnel facility as the study of thermals in crossflow and the details of the measurements were the same.⁵⁴ The only change was that the source flow was maintained throughout the time period where measurements were made, in order to simulate starting plumes as opposed to thermals which involved interrupted source flows.

The test conditions for the studies of starting plumes in uniform crossflow can be summarized as follows: source diameters of 3.2 and 6.4 mm, source densities of 1071 and 1198 kg/m³, ambient densities of 998 kg/m³, source Reynolds numbers of 4000-11000, source Froude numbers of 14-82, and ratios of source/crosstream flow velocities of 5-35.

Theoretical Methods

Similar to the analysis of thermals in uniform crossflow that was discussed earlier, two key assumptions were made to treat starting plumes in uniform crossflow, both of which were motivated by the treatment of steady plumes in uniform crossflow due to Baum et al.,¹ namely: (1) the crossflow motion was assumed to approximate no-slip convective flow, and (2) the vertical motion was assumed to approximate the penetration properties of a starting plume in a still and uniform environment. The configuration for the present analysis of starting plumes in a uniform crossflow is illustrated in Fig. 22. The source flow enters from a passage having a diameter, d , a density, ρ_o , and velocity, u_o , and flows into an environment having a density, ρ_∞ , and a uniform crossflow velocity, u_∞ ; the properties of interest include the maximum vertical, crossflow (horizontal) and radial penetration

distances, x_p , y_p and r_p , illustrated in Fig. 22. Major assumptions are similar to those used earlier for thermals in crossflow, as follows: physical property variations are small (i.e., the flows are weakly buoyant so that density variations are linear functions of the degree of mixing as discussed earlier for starting plumes in still environments), sources are assumed to start instantly and subsequently to maintain a constant flow rate (using an extrapolated temporal origin to handle the actual start process similar to starting plumes in still environments), virtual origins are used in both the vertical and crosstream directions to maximize conditions where self-preserving behavior is observed, the crosstream motion is assumed to satisfy the no-slip convection approximation, and the vertical motion is assumed to approximate the penetration properties of a starting plume in a still and uniform environment.

Under these assumptions at this limit, the maximum vertical penetration properties approximate a starting plume in a still environment and are given by Eqs. (19), (24), (25) and (26), the maximum radial penetration distance is given by Eq. (20), and the maximum penetration of the crossflow (horizontal) direction is given by Eq. (25) similar to the earlier treatment of thermals in crossflow under similar assumptions. In addition, Eqs. (4) and (5) can be used to find ℓ_M/d and Fr_o , similar to a starting plume in a still environment under present approximations.

Results and Discussion

Study of starting plumes in crossflow is still in progress in this laboratory; therefore, the following description only represents a progress report about the limited results obtained thus far.

The maximum crosstream (horizontal) penetration distances of starting

plumes in uniform crossflow satisfied the no-slip convection approximation of Eq. (27), similar to the behavior of thermals in uniform crossflows as discussed in connection with Fig. 18. In addition, the virtual origin in the crosstream direction was essentially zero, similar to earlier findings for thermals in uniform crossflow.

The normalized maximum vertical penetration distances of starting plumes in crossflow at weak crossflow conditions are plotted according to the self-preserving scaling of Eqs. (19) and (24), (25) and (27) in Figs. 23 and 24. These measurements generally behave very similar to starting plumes in still environments for this coordinate direction, with $n=3/4$. Thus, self-preserving scaling is reached for dimensionless times $(t-t_d)/t^* > 200$ which corresponds to $(x_p-x_o)/d > 40$ and $(x_p-x_o)/\ell_M > 5$. As mentioned earlier in connection with starting plumes in still environments, these conditions are much closer to the source than is required to reach self-preservation of the structure properties of steady plumes in still environments, showing that self-preserving conditions for various properties are reached at different distances from the source.

The normalized maximum radial penetration distances of starting plumes in uniform crossflow are plotted according to the self-preserving scaling of Eq. (20) in Fig. 25 in terms of the dimensionless vertical penetration distance. Similar to the other flows that have been considered, the normalized radial penetration distance decreases with increasing streamwise distance and becomes relatively constant in the self-preserving region where $(x_p-x_o)/d \geq 40$ with $C_r = 0.16$, similar to starting plumes in still environments. In addition, measurements plotted according to the normalized expression for the vertical

penetration distances in terms of the horizontal penetration distance from Eq. (33) are illustrated in Fig. 25. As discussed elsewhere, approach of vertical penetration to self-preserving behavior clearly is similar to the approach of radial penetration to self-preserving behavior. In addition, the location of the virtual origin was measured yielding $x_o/d = -20$ which is very similar to findings for the other flows that have been studied using the salt-water simulations.

Finally, the various properties of starting plumes in crossflow are summarized in Table 4. Most of the properties of starting plumes in still environments (see Table 3) and in crossflow are the same, indicating that crossflow has only a mild effect on the vertical and radial penetration properties of starting plumes.

Conclusions

The properties of round turbulent starting plumes in uniform crossflow were reviewed. This work is in progress, however, so that available measurements are limited. The major conclusions of these considerations are as follows:

1. The flows became turbulent within 5 diameters from the source, and achieved self-preserving behavior for $(x_p - x_o)/d \geq 40$ and $(x_p - x_o)/\ell_M \geq 5$.
2. Within the self-preserving region, vertical dimensionless penetration distances generally varied as a function of time in accord with behavior expected for self-preserving starting plumes in crossflow, e.g., varying according to dimensionless time to the 3/4 power.
3. Throughout the entire range of observations, the no-slip convection approximation for starting plumes in weak

crossflow was satisfactory, yielding a simple and convenient way of estimating flow trajectories.

4. The radial penetration distances of starting plumes in weak crossflow satisfied the same general scaling relationships observed for starting plumes in still environments, with $C_r = 0.16$ in both cases.

5. The virtual origins of starting plumes in both crossflow and in a still environment were the same, with $y_o/d = -20$.

CONCLUDING REMARKS

The findings of the present review suggest that significant progress has been made toward gaining a better understanding of round buoyant turbulent thermals and plumes in unstratified still and crossflowing environments. The main observations are that achieving self-preserving behavior depends upon the flow and the property under consideration; that complete self-preserving behavior is achieved farther from the source and generally involves narrower scaled flow widths than previously thought; that thermal and plume motion due to crossflow satisfies the no-slip convection approximation; and that salt-water simulations appear to provide results at laboratory scale that are relevant large-scale practical flows. Many issues about these flows, however, still must be resolved: the structure and mixing properties of unsteady thermals and plumes are not well understood due to problems of making measurements of transient flows; the structure and mixing properties of steady plumes in crossflow are not well understood due to problems of making measurements in three-dimensional flows; the behavior of buoyant turbulent flows in stratified environments has received very little attention so that even simple flow penetration measurements for this flow

would be helpful; and baseline information about the penetration, structure and mixing properties of turbulent nonbuoyant puffs and jets should be developed in order to better understand effects of buoyancy present in corresponding turbulent buoyant thermals and plumes.

ACKNOWLEDGMENTS

The authors' research concerning buoyant turbulent flows is supported by the United States Department of Commerce, National Institute of Standards and Technology, Grant Nos. 60NANB8D0081 and 60NANB1D006, with H.R. Baum of the Building and Fire Research Laboratory serving as Scientific Officer; L.P. Bernal and L.-K. Tseng also contributed to this research.

REFERENCES

- ¹Baum, H.R., McGrattan, K.B., and Rehm, R.G., "Simulation of Smoke Plumes from Large Pool Fires," Proc. Combust. Inst., Vol. 25, 1994, pp. 1463-1469.
- ²Baum, H.R., McGrattan, K.B., and Rehm, R.G., "Mathematical Modeling and Computer Simulation of Fire Phenomena," *Fire Safety Science-Proceedings of the Fourth International Symposium*, International Association of Fire Safety Science, Boston, 1994, pp. 185-193.
- ³Baum, H.R., "Modeling and Scaling Laws for Large Fires," AIAA Paper No. 2002-2886, 2002.
- ⁴Turner, J.S., "Buoyant Plumes and Thermals," Ann. Rev. Fluid Mech., Vol. 1, 1969, pp. 29-44.
- ⁵Turner, J.S., *Buoyancy Effects in Fluids*, Cambridge University Press, Cambridge, London, 1973.
- ⁶Tennekes, H., and Lumley, J.L., *A First Course in Turbulence*, MIT Press, Cambridge, Massachusetts, 1972, pp. 113-124.
- ⁷Hinze, J.O., *Turbulence*, 2nd Ed., McGraw-Hill, New York, 1975, pp. 534-585.
- ⁸Chen, C.J., and Rodi, W., *Vertical Turbulent Buoyant Jets: A Review of Experimental Data*, Pergamon Press, Oxford, 1980.
- ⁹List, E.J., "Turbulent Jets and Plumes," Ann. Rev. Fluid Mech., Vol. 14, 1982, pp. 189-212.
- ¹⁰Rouse, H., Yih, C.S., and Humphreys, H.W., "Gravitational Convection from a Boundary Source," Tellus, Vol. 4, 1952, pp. 201-210.
- ¹¹Morton, B.R., Taylor, G.I., and Turner, J.S., "Turbulent Gravitational Convection from Maintained and Instantaneous Sources," Proc. Roy. Soc. London, Vol. A234, Part 1, 1956, pp. 1-23.
- ¹²Morton, B.R., "Forced Plumes," J. Fluid Mech., Vol. 5, 1959, pp. 151-163.
- ¹³Abraham, G., "Jet Diffusion in Liquid of Greater Density," ASCE J. Hyd. Div., Vol. 86, 1960, pp. 1-13.
- ¹⁴Seban, R.A., and Behnia, M.M., "Turbulent Buoyant Jets in Unstratified Surroundings," Int. J. Heat Mass Trans., Vol. 19, 1976, pp. 1197-1204.
- ¹⁵George, W.K., Jr., Alpert, R.L., and Tamanini, F., "Turbulence Measurements in

an Axisymmetric Buoyant Plume,” Int. J. Heat Mass Trans., Vol. 20, 1977, pp. 1145-1154.

¹⁶Zimin, V.D., and Frik, P.G., “Average Temperature Fields in Asymmetrical Turbulent Streams over Localized Heat Sources,” Izv. Akad. Nauk. SSSR, Mekhanika Zhidkosti Gaza, Vol. 2, 1977, pp. 199-203.

¹⁷Kotsovinos, N.E., and List, E.J., “Turbulent Buoyant Jets. Part 1. Integral Properties,” J. Fluid Mech., Vol. 81, 1977, pp. 25-44.

¹⁸Mizushima, T., Ogino, F., Veda, H., and Komori, S., “Application of Laser-Doppler Velocimetry to Turbulence Measurements in Non-Isothermal Flow,” Proc. Roy. Soc. London, Vol. A366, 1979, pp. 63-79.

¹⁹Ogino, F., Takeuchi, H., Kudo, I., and Mizushima, T., “Heated Jet Discharged Vertically in Ambients of Uniform and Linear Temperature Profiles,” Int. J. Heat Mass Trans., Vol. 23, 1980, pp. 1581-1588.

²⁰Kotsovinos, N.E., “Temperature Measurements in a Turbulent Round Plume,” Int. J. Heat Mass Trans., Vol. 28, 1985, pp. 771-777.

²¹Papanicolaou, P.N., and List, E.J., “Statistical and Spectral Properties of Tracer Concentration in Round Buoyant Jets,” Int. J. Heat Mass Trans., 1987, Vol. 30, pp. 2059-2071.

²²Papanicolaou, P.N., and List, E.J., “Investigation of Round Vertical Turbulent Buoyant Jets,” J. Fluid Mech., Vol. 195, 1988, pp. 341-391.

²³Papantoniou, D., and List, E.J., “Large Scale Structure in the Far Field of Buoyant

Jets,” J. Fluid Mech., Vol. 209, 1989, pp. 151-190.

²⁴Shabbir, A., and George, W.K., “Experiments on a Round Turbulent Buoyant Plume,” NASA Technical Memorandum 105955, 1992.

²⁵Peterson, J., and Bayazitoglu, Y., “Measurements of Velocity and Turbulence in Vertical Axisymmetric Isothermal and Buoyant Plumes,” J. Heat Trans., Vol. 114, 1992, pp. 135-142.

²⁶Panchapakesan, N.R., and Lumley, J.L., “Turbulence Measurements in Axisymmetric Jets of Air and Helium. Part 1. Air Jet,” J. Fluid Mech., Vol. 246, Part 1, 1993, pp. 197-223.

²⁷Panchapakesan, N.R., and Lumley, J.L., “Turbulence Measurements in Axisymmetric Jets of Air and Helium. Part 2. Helium Jet,” J. Fluid Mech., Vol. 246, Part 2, 1993, pp. 225-247.

²⁸Dai, Z., Tseng, L.-K., and Faeth, G.M., “Structure of Round, Fully-Developed, Buoyant Turbulent Plumes,” J. Heat Trans., Vol. 116, No. 2, 1994, pp. 409-417.

²⁹Dai, Z., Tseng, L.-K., and Faeth, G.M., “Velocity Statistics of Round, Fully-Developed Buoyant Turbulent Plumes,” J. Heat Transfer, Vol. 117, No. 1, 1995, pp. 138-145.

³⁰Dai, Z., Tseng, L.-K., and Faeth, G.M., “Velocity/Mixture-Fraction Statistics of Round, Self-Preserving Buoyant Turbulent Plumes,” J. Heat Trans., Vol. 117, No. 4, 1995, pp. 918-926.

³¹Dai, Z., and Faeth, G.M., “Measurements of the Structure of Self-Preserving Round

Buoyant Turbulent Plumes,” J. Heat Trans., Vol. 118, No. 2, 1996, pp. 493-495.

³²Wu, J.-S., and Faeth, G.M., “Sphere Wakes in Still Surroundings at Intermediate Reynolds Numbers,” AIAA J., Vol. 31, No. 8, 1993, pp. 1448-1455.

³³Becker, H.A., Hottel, H.C., and Williams, G.C., “The Nozzle-Fluid Concentration Field of the Round, Turbulent, Free Jet,” J. Fluid Mech. Vol. 30, 1967, pp. 285-303.

³⁴Pivovarov, M.A., Zhang, H., Ramaker, D.E., Tatem, P.A., and Williams, F.W., “Similarity Solutions in Buoyancy-Controlled Diffusion Flame Modelling,” Combust. Flame, Vol. 92, 1992, pp. 308-319.

³⁵Dai, Z., “The Structure of Self-Preserving Round Buoyant Turbulent Plumes,” Ph.D. Thesis, The University of Michigan, Ann Arbor, Michigan, 1995.

³⁶Scorer, R.S., “Experiments in Connection With Isolated Masses of Buoyant Fluid,” J. Fluid Mech., Vol. 2, 1957, pp. 583-594.

³⁷Turner, J.S., “The Dynamics of Spheroidal Masses of Buoyant Fluid,” J. Fluid Mech., Vol. 19, 1964, pp. 481-490.

³⁸Richards, J.M., “Puff Motions in Unstratified Surroundings,” J. Fluid Mech., Vol. 21, Part 1, 1965, pp. 97-106.

³⁹Fay, J.A., and Lewis, D.H., “Unsteady Burning of Unconfined Fuel Vapor Clouds,” Proc. Combust. Inst., Vol. 16, 1976, pp. 1397-1405.

⁴⁰Batt, R.G., Brigoni, R.A., and Rowland, D.J., “Temperature-Field Structure Within Atmospheric Buoyant Thermals,” J. Fluid Mech., Vol. 141, 1984, pp. 1-25.

⁴¹Thompson, R.S., Snyder, W.H., and Weil, J.C., “Laboratory Simulation of the Rise of Buoyant Thermals Created by Open Detonation,” J. Fluid Mech., Vol. 417, 2000, pp. 127-156.

⁴²Turner, J.S., “Buoyant Vortex Rings,” Proc. Roy. Soc., London, Vol. A239, 1957, pp. 61-75.

⁴³Morton, B.R., “Weak Thermal Vortex Rings,” J. Fluid Mech., Vol. 9, 1960, pp. 107-118.

⁴⁴Sangras, R., Kwon, O.C., and Faeth, G.M., “Self-Preserving Properties of Unsteady Round Nonbuoyant Turbulent Starting Jets and Puffs in Still Fluids,” J. Heat Trans., Vol. 124, No. 1, 2002, pp. 1-24.

⁴⁵Diez, F.J., Kwon, O.C., Sangras, R. and Faeth, G.M., “Self-Preserving Properties of Unsteady Round Turbulent Buoyant Plumes and Thermals in Still Fluids,” J. Heat Trans., submitted.

⁴⁶Steckler, K.D., Baum, H.R., and Quintiere, J.G., “Salt Water Modeling of Fire Induced Flows in Multicomponent Enclosures,” Proc. Combust. Inst., Vol. 21, 1986, pp. 143-149.

⁴⁷Wu, P.-K., Miranda, R.F., and Faeth, G.M., “Effects of Initial Flow Conditions on Primary Breakup of Nonturbulent and Turbulent Round Liquid Jets,” Atomization and Sprays, Vol. 5, 1995, pp. 175-196.

⁴⁸Lange, N.A., *Handbook of Chemistry*, Handbook Publishers, Sandusky, Ohio, 1952, p. 1160.

⁴⁹Turner, J.S., “The Starting Plume in Neutral Surroundings,” J. Fluid Mech., Vol. 13, 1962, pp. 356-368.

⁵⁰Faeth, G.M., “Spray Combustion Phenomena,” Proc. Combust. Inst., Vol. 26, 1996, pp. 1593-1612.

⁵¹Middleton, J.H., “The Asymptotic Behavior of a Starting Plume,” J. Fluid Mech., Vol. 72, 1975, pp. 753-771.

⁵²Delichatsios, M.A., “Time Similarity Analysis of Unsteady Buoyant Plumes,” J. Fluid Mech., Vol. 93, 1979, pp. 241-250.

⁵³Pantzlaff, L., and Lueptow, R.M., “Transient Positively and Negatively Buoyant Turbulent Round Jets,” Experiments in Fluids, Vol. 27, 1999, pp. 117-125.

⁵⁴Diez, F.J., Kwon, O.C., Sangras, R., Bernal, L.P., and Faeth, G.M., “Round Turbulent Puffs and Buoyant Thermals in Uniform Crossflows,” AIAA Paper No. 2002-2773, 2002.

⁵⁵Andreopoulos, J., “Heat Transfer Measurements in a Heated Jet-Pipe Flow Issuing into a Cold Cross Stream,” Phys. Fluids, Vol. 26, No. 4, 1983, pp. 3200-3210.

⁵⁶Alton, B.W., Davidson, G.A., and Slawson, P.R., “Comparison of Measurements and Integral Model Predictions of Hot Water Plume Behavior in a Crossflow,” Atmos. Environ. A.-Gen., Vol. 27A, No. 4, 1993, pp. 589-598.

⁵⁷Hasselbrink, E.F., and Mungal, M.G., “Observations on the Stabilization Region of Lifted Non-Premixed Methane Transverse Jet Flames,” Proc. Combust. Inst., Vol. 27, 1998, pp. 1167-1173.

⁵⁸Hinze, J.O., *Turbulence*, 2nd ed., McGraw-Hill, New York, 1975, pp. 175-319.

Table 1. Summary of self-preserving buoyant turbulent plume properties.^a

| Parameter | Dai et al. ^{28,31} | Papanicolaou & List ²² | Papanicolaou & List ²¹ | Shabbir & George ²⁴ | George et al. ¹⁵ | Ogino et al. ¹⁹ |
|------------------------|-----------------------------|-----------------------------------|-----------------------------------|--------------------------------|-----------------------------|----------------------------|
| Medium | gas | liquid | liquid | gas | gas | liquid |
| $(x-x_0)/d$ | 87-151 | 22-62 | 12-20 | 10-25 | 8-16 | 6-36 |
| $(x-x_0)/\ell_M$ | 12-43 | 9-62 | > 5 | 6-15 | 6-12 | 5-15 |
| k_z^2 | 125 | 80 | 80 | 68 | 65 | --- |
| $\ell_f/(x-x_0)$ | 0.09 | 0.11 | 0.11 | 0.12 | 0.19 | --- |
| $F(0)$ | 12.6 | 14.3 | 11.1 | 9.4 | 9.1 | --- |
| $(\bar{f}'/\bar{f})_c$ | 0.45 | 0.40 | 0.40 | 0.40 | 0.40 | --- |
| k_z^2 | 93 | 90 | 58 | 55 | 51 | --- |
| $\ell_u/(x-x_0)$ | 0.10 | 0.11 | --- | 0.13 | 0.14 | 0.14 |
| $U(0)$ | 4.3 | 3.9 | --- | 3.4 | 3.4 | 3.4 |
| $(\bar{u}'/\bar{u})_c$ | 0.22 | 0.25 | --- | 0.32 | 0.28 | --- |
| E_0 | 0.086 | 0.080 | --- | 0.109 | 0.112 | 0.117 |

^aRound buoyant turbulent plumes in still and unstratified environments. Range of streamwise distances are for conditions where quoted self-preserving properties were found from measurements over the cross section of the plumes. Entries are ordered in terms of decreasing k_z .

Table 3. Summary of self-preserving buoyant turbulent starting plume properties^a

| Source | Medium | $(x_p-x_0)/d^b$ | Re_0 | n | C_s | C_t |
|---------------------------|--------|-----------------|------------|-----|-------|-------------|
| Diez et al. ⁴⁵ | liquid | 110 | 6000-12000 | 3/4 | 2.80 | 0.15 |
| Turner ⁴⁹ | liquid | --- | --- | 3/4 | --- | 0.18 ± 0.03 |

^aInjection of round turbulent buoyant starting plumes into still and unstratified environments.
^bMaximum vertical penetration distance observed.

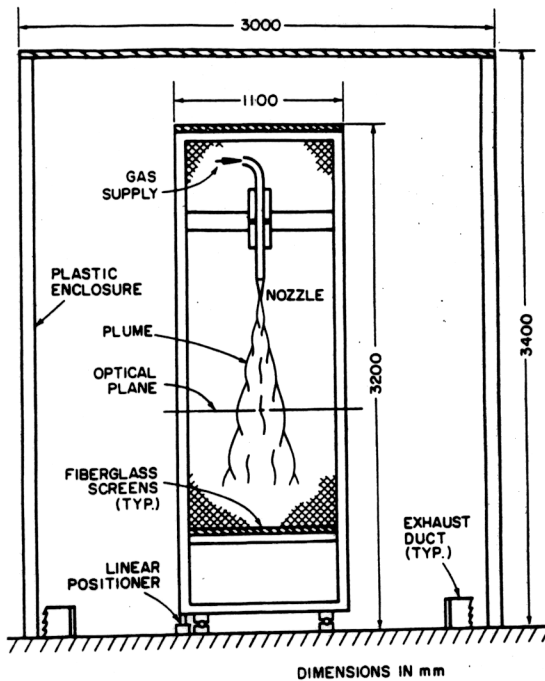


Fig. 1. Sketch of the test apparatus for steady plumes in still environments. From Dai et al.²⁸

Table 2. Summary of self-preserving buoyant turbulent thermal properties^a

| Parameter | Diez et al. ⁴⁵ | Score ³⁶ | Turner ²⁷ | Thompson et al. ⁴¹ |
|-----------------|---------------------------|---------------------|----------------------|-------------------------------|
| Medium | liquid | liquid | liquid | liquid |
| $(x_p-x_0)/d^b$ | 100 | --- | --- | --- |
| $Q_0/(A_0 d)$ | 50-382 | --- | --- | --- |
| Re_0 | 6000-12000 | --- | --- | --- |
| n | 1/2 | 1/2 | 1/2 | --- |
| C_s | 2.10 | --- | --- | --- |
| C_t | 0.19 | 0.26 | 0.25 | 0.24 |

^aInjection of round turbulent buoyant thermals into still and unstratified environments.
^bMaximum vertical penetration distance observed.

Table 4. Summary of self-preserving buoyant turbulent flows in uniform crossflow.^a

| Medium | $(x_p-x_0)/d^b$ | $Q_0/(A_0 d)^c$ | x_0/d | Re_0 | n | C_s | C_t |
|--|-----------------|-----------------|---------|------------|-----|-------|-------|
| Thermals, from Diez et al. ⁴⁴ | | | | | | | |
| liquid | 200 | 18-318 | -20 | 6000-12000 | 1/2 | 2.0 | 0.14 |
| Starting plumes, from present study: | | | | | | | |
| liquid | 200 | --- | -20 | 6000-12000 | 3/4 | 2.8 | 0.16 |

^aBoth flows satisfied the no-slip convection approximation in the crossflow (horizontal) direction with $y_0/d = 0$.
^bMaximum vertical penetration distance observed.

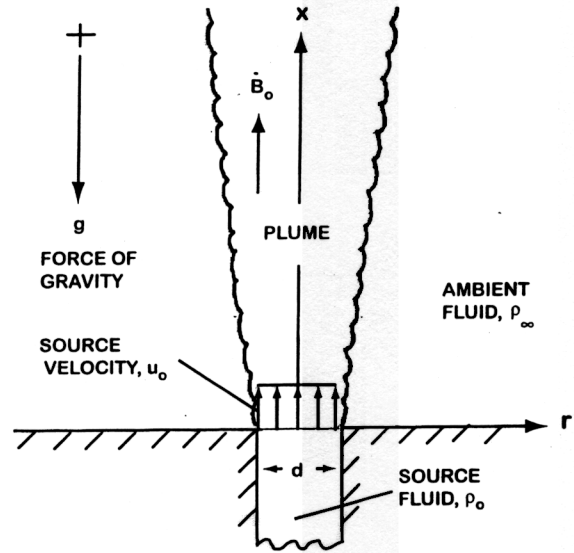


Fig. 2. Sketch of a steady plume in a still environment.

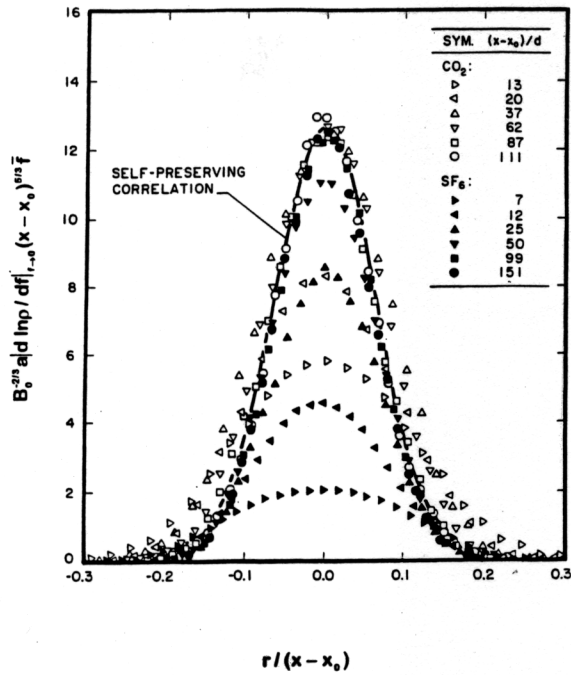


Fig. 3. Development of radial distributions of mean mixture fractions as a function of distance from the source for steady plumes in still environments. From Dai et al.²⁸

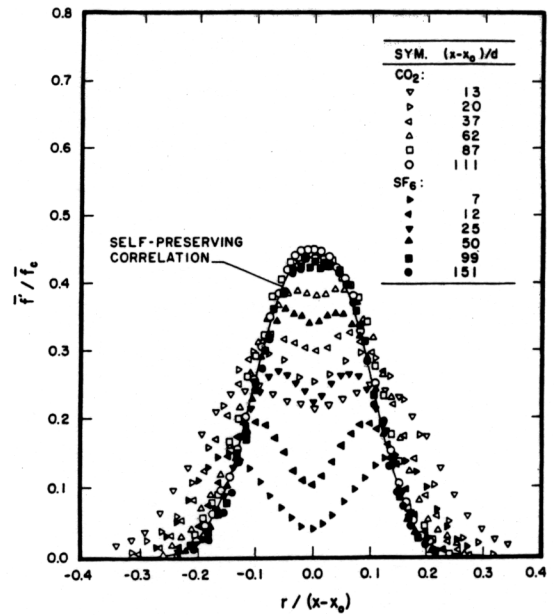


Fig. 4. Development of radial distributions of rms mixture fraction fluctuations as a function of distance from the source for steady plumes in still environments. From Dai et al.²⁸

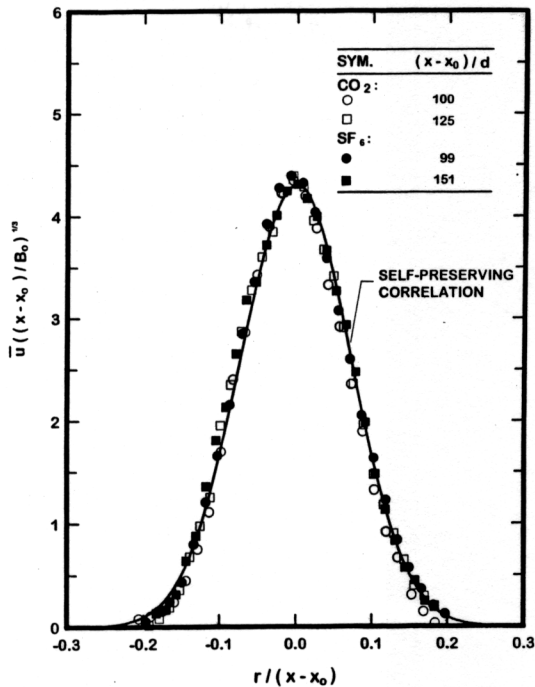


Fig. 5. Radial distributions of mean streamwise velocities for self-preserving steady plumes in still environments. From Dai et al.²⁹

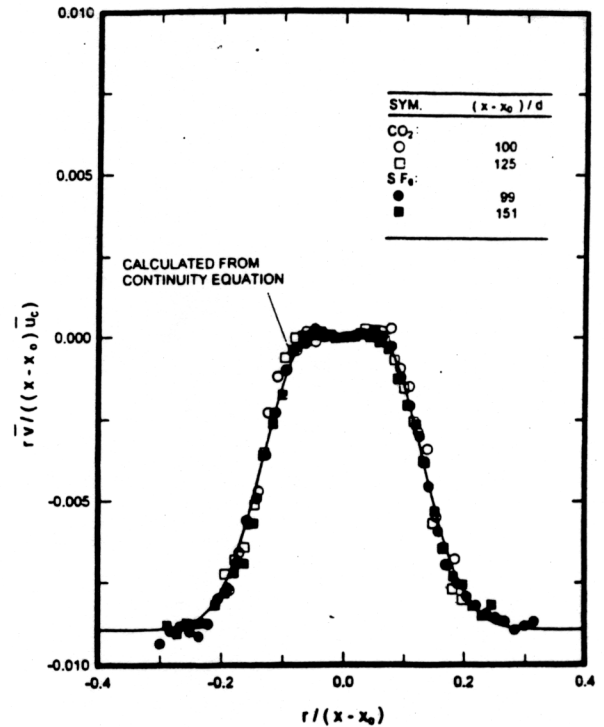


Fig. 6. Radial distributions of mean radial velocities for self-preserving steady plumes in still environments. From Dai et al.²⁹

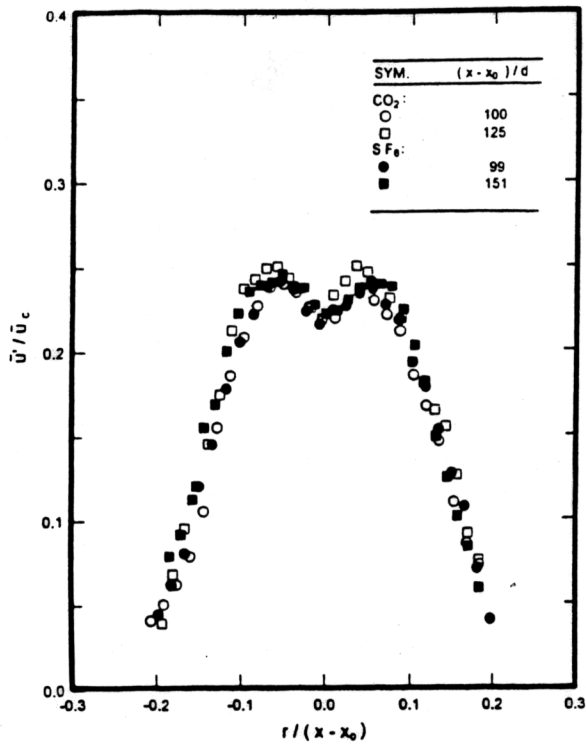


Fig. 7. Radial distributions of streamwise rms velocity fluctuations for self-preserving steady plumes in still environments. From Dai et al.²⁹

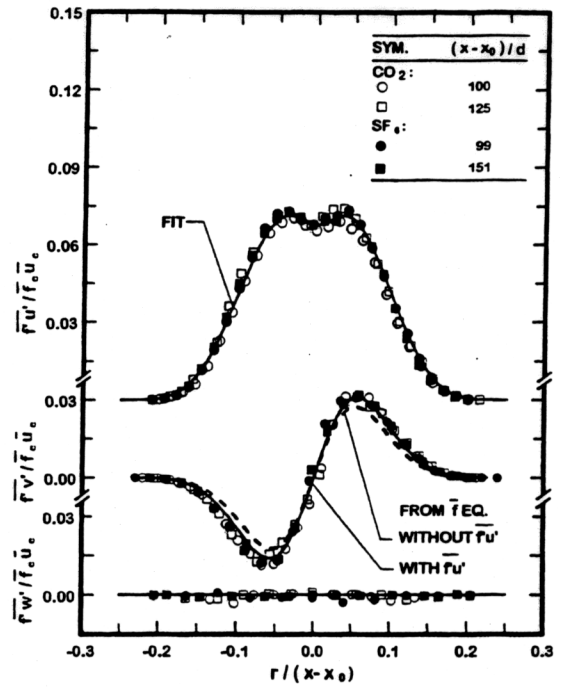


Fig. 8. Radial distributions of turbulent mass fluxes for self-preserving steady plumes in still environments. From Dai et al.³⁰

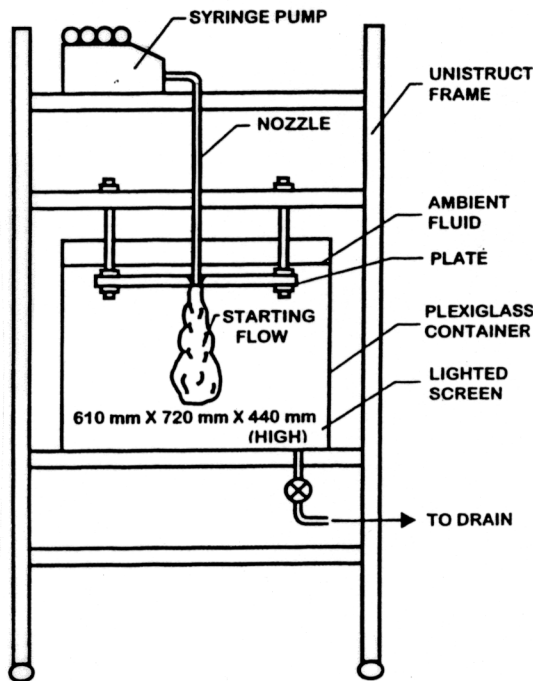


Fig. 9. Sketch of the test apparatus for thermals and starting plumes in still environments. From Sangras et al.⁴⁴

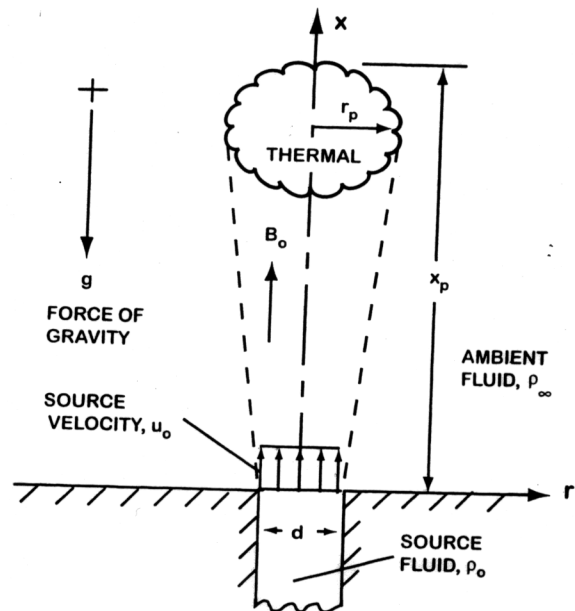


Fig. 10. Sketch of a thermal in a still environment. From Diez et al.⁴⁵

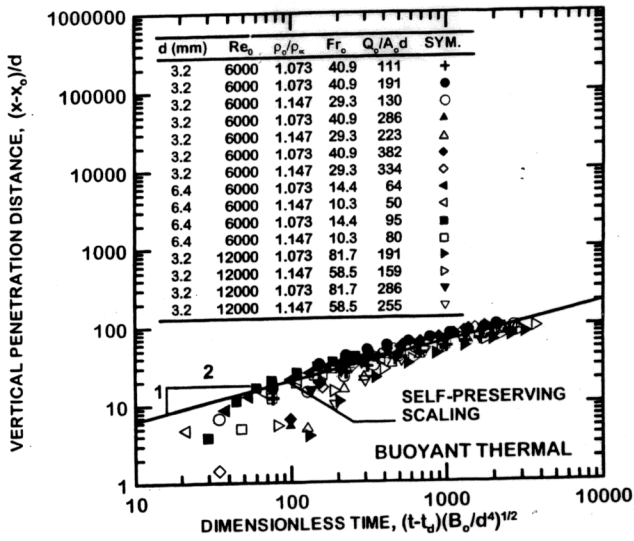


Fig. 11. Maximum vertical penetration distances as a function of time for thermals in still environments. From Diez et al.⁴⁵

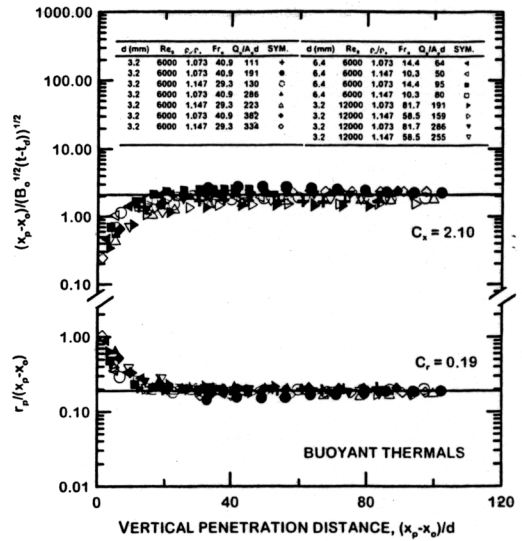


Fig. 12. Maximum radial and normalized vertical penetration distances as a function of maximum vertical penetration distances for thermals in still environments. From Diez et al.⁴⁵

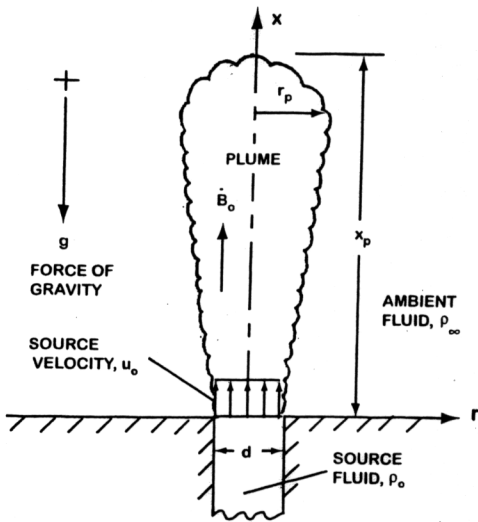


Fig. 13. Sketch of a starting plume in a still environment. From Diez et al.⁴⁵

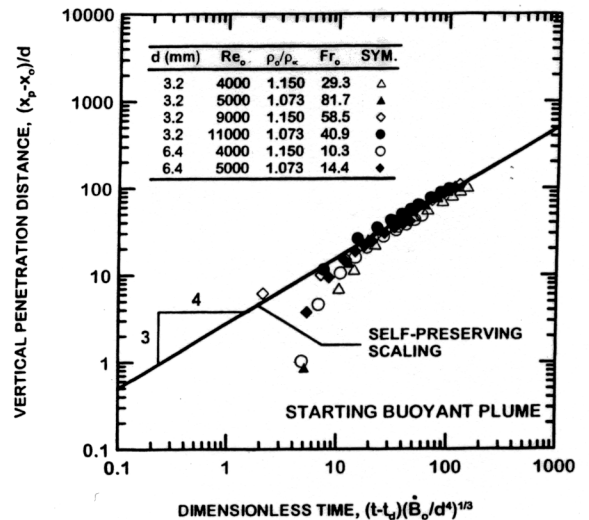


Fig. 14. Maximum vertical penetration distances as a function of time for starting plumes in still environments. From Diez et al.⁴⁵

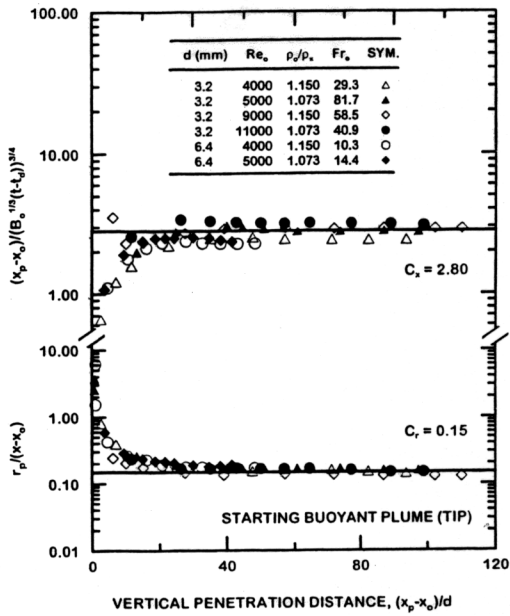


Fig. 15. Maximum radial and normalized vertical penetration distances as a function of maximum vertical penetration distances for starting plumes in still environments. From Diez et al.⁴⁵

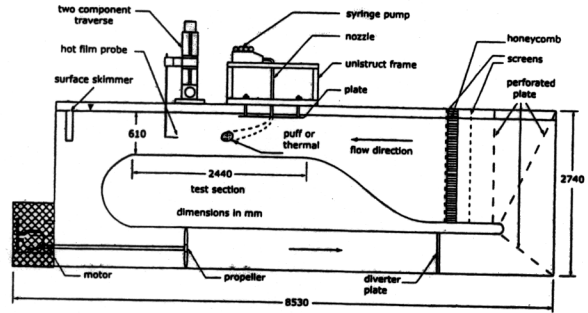


Fig. 16. Sketch of the test apparatus for thermals and starting plumes in uniform crossflow. From Diez et al.⁴⁵

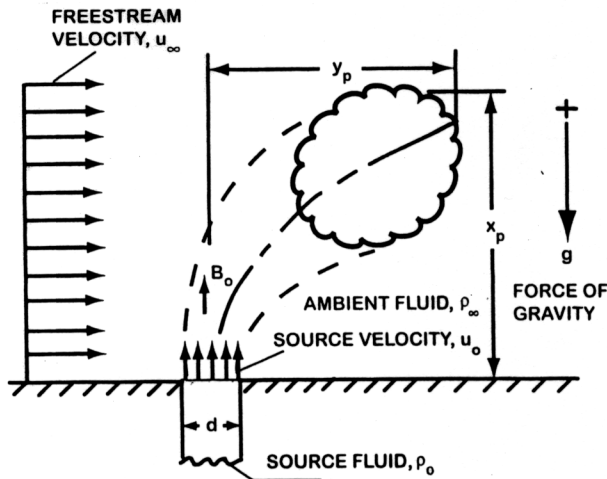


Fig. 17. Sketch of a thermal in a uniform crossflow. From Diez et al.⁴⁵

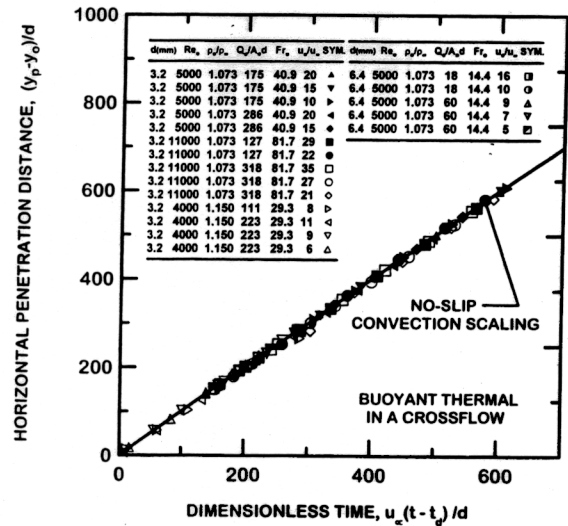


Fig. 18. Maximum crossflow penetration distances as a function of time for thermals in uniform crossflow. From Diez et al.⁵⁴

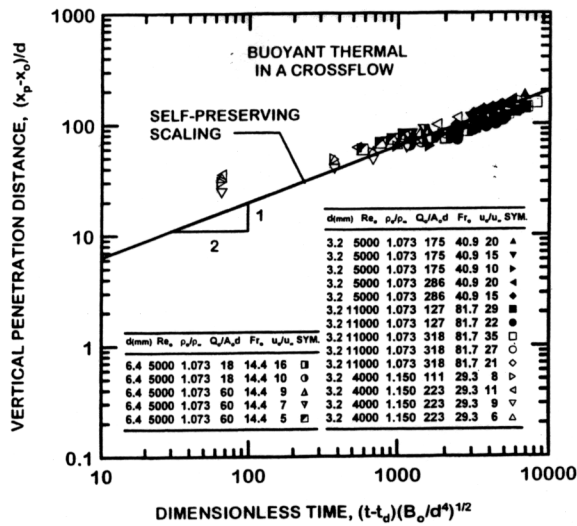


Fig. 19. Maximum vertical penetration distances as a function of time for thermals in uniform crossflow. From Diez et al.⁵⁴

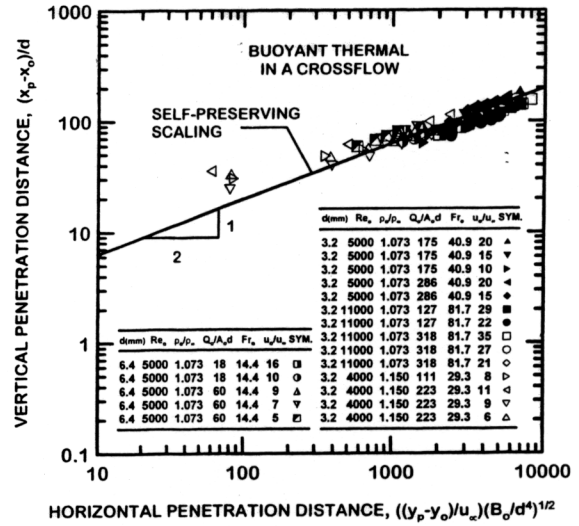


Fig. 20. Maximum vertical penetration distances as a function of maximum crossstream penetration distances for thermals in uniform crossflow. From Diez et al.⁵⁴

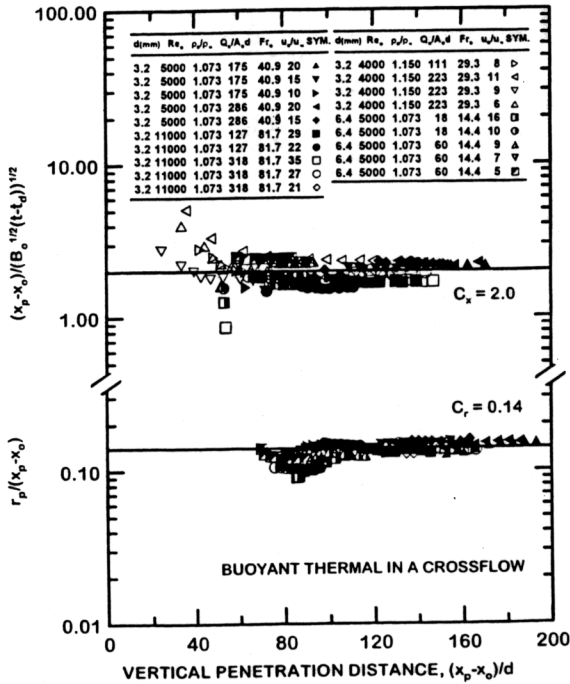


Fig. 21. Maximum radial and normalized vertical penetration distances as a function of maximum vertical penetration distances for thermals in uniform crossflow. From Diez et al.⁵⁴

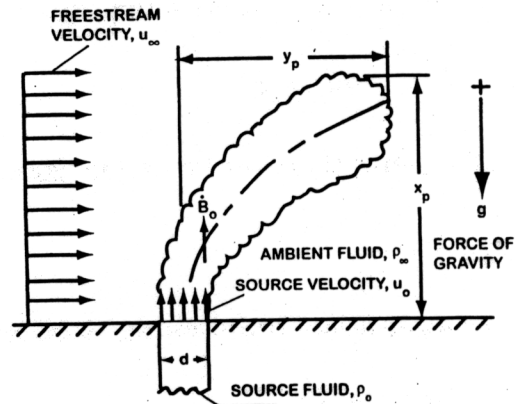


Fig. 22. Sketch of a starting plume in a uniform crossflow.

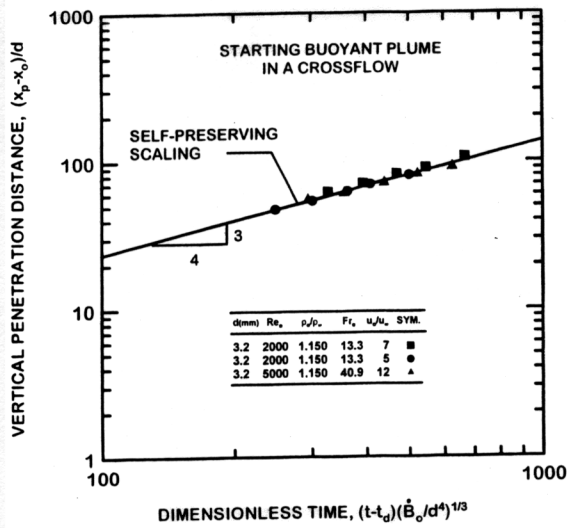


Fig. 23. Maximum vertical penetration distances as a function of time for starting plumes in uniform crossflow at weak crossflow conditions.

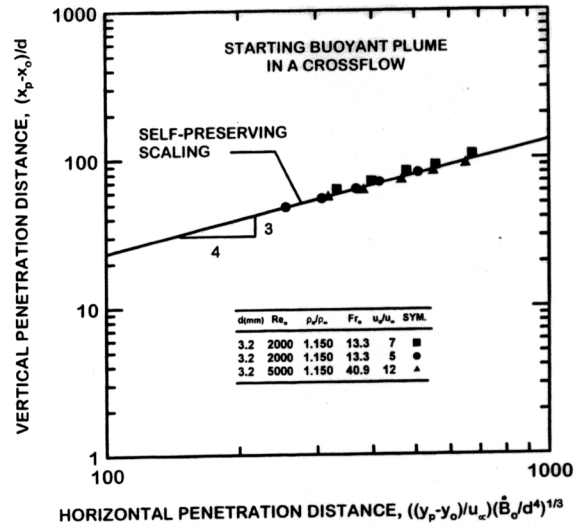


Fig. 24. Maximum vertical penetration distances as a function of maximum horizontal penetration distances for starting plumes in uniform crossflow at weak crossflow conditions.

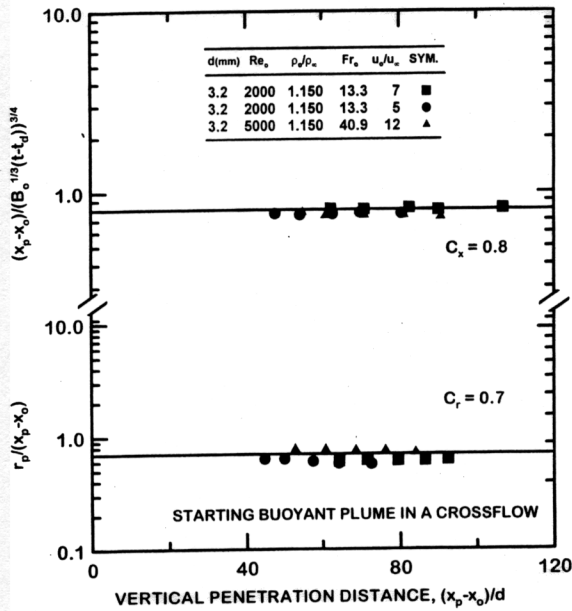


Fig. 25. Maximum radial and normalized vertical penetration distances as a function of maximum vertical penetration distances for starting plumes in uniform crossflow at weak crossflow conditions.